Preliminary analysis and hanger adjustment of tied arch bridges
by William Edward Beyer

A thesis submitted in partial fulfillment of the requirements for the degree of Master of Science in Engineering Mechanics
Montana State University

Abstract:
Preliminary design of a tied arch bridge is complex due to the many possible parameters of the problem. After obtaining a design the minimization of dead load moment is an important consideration. Similarly, obtaining proper tensions in the hangers of a tied arch bridge is very important, to prevent overstressing of the arch.

By using matrix structural analysis, the effects of certain parameters upon tied arch behavior are investigated. The parameters include rise to span ratio, hanger spacing, ratio of areas of rib and tie, and ratio of moments of inertia of rib and tie. The geometry of an existing span was used for analysis.

The results of the parametric study are portrayed graphically for a range of the parameters. Methods for analysis of dead load moment and hanger tension adjustment are developed. Finally a preliminary design example is considered.

PRELIMINARY ANALYSIS AND HANGER ADJUSTMENT OF TIED ARCH BRIDGES

by

William Edward Beyer

A thesis submitted in partial fulfillment
of the requirements for the degree

of

Master of Science

in

Engineering Mechanics

MONTANA STATE UNIVERSITY
Bozeman, Montana

May 1984

APPROVAL

of a thesis submitted by

William Edward Beyer

This thesis has been read by each member of the thesis committee and has been found to be satisfactory regarding content, English usage, format, citations, bibliographic style, and consistency, and is ready for submission to the College of Graduate Studies.

May 23, 1984
Date

Fred F Uhlen
Chairperson, Graduate Committee

Approved for the Major Department

May 23, 1984
Date

Fred F Uhlen
Head, Major Department

Approved for the College of Graduate Studies

June 1, 1984
Date

Henry L Parsons
Graduate Dean

STATEMENT OF PERMISSION TO USE

In presenting this thesis in partial fulfillment of the requirements for a master's degree at Montana State University, I agree that the Library shall make it available to borrowers under the rules of the Library. Brief quotations from this thesis are allowable without special permission, provided that accurate acknowledgement of the source is made.

Permission for extensive quotation from or reproduction of this thesis may be granted by my major professor, or in his absence, by the Director of Libraries when, in the opinion of either, the proposed use of the material is for scholarly purposes. Any copying or use of the material in this thesis for financial gain shall not be allowed without my written permission.

Signature William E. Beyer

Date May 22, 1984

ACKNOWLEDGMENTS

The author wishes to express his appreciation to Dr. F. F. Videon for his guidance, assistance, and encouragement during the preparation of this thesis.

The author also wishes to thank the following individuals and consulting firms for their assistance:

Maurice D. Miller, Howard Needles Tammen & Bergendoff
Kansas City, MO

Sherwood Richardson, Richardson, Gordon and Associates
Pittsburgh, PA

Eugene A. Halupnik, Cuyahoga County Bridge Engineer
Cleveland, OH

Donald J. MacDougall, U.S. Steel American Bridge Division
Pittsburgh, PA

F. P. Blanchard, Sverdrup, Parcel & Associates
St. Louis, MO

Richard P. Knight, Bethlehem Steel Corporation
Bethlehem, PA

Louis G. Silano, Parsons, Brinckerhoff, Quade & Douglas
New York, NY

TABLE OF CONTENTS

	Page
APPROVAL	ii
STATEMENT OF PERMISSION TO USE	iii
ACKNOWLEDGMENTS	iv
TABLE OF CONTENTS	v
LIST OF TABLES	vii
LIST OF FIGURES	ix
ABSTRACT	xii
I. INTRODUCTION	1
Description	1
History	1
II. MINIMIZATION OF DEAD LOAD MOMENTS IN A TIED ARCH	7
The principle of moment minimization	7
Application of the principle to a frame example	7
Application of the principle to a tied arch	11
Computer analysis	18
III. HANGER TENSION ADJUSTMENT	23
Methods of determining hanger tension	24
Force-deflection method	24
Frequency of vibration method	25
Strain gages	27
Analysis	28
IV. EFFECTS OF VARIOUS PARAMETERS UPON TIED ARCH BEHAVIOR	35
Discussion of parameters	35
Rib and tie moment influence lines	41
Hanger forces	59
Rib and tie deflection	64
Proportion of live load moment carried by the rib and by the tie	68

TABLE OF CONTENTS--Continued

	Page
V. PRELIMINARY ANALYSIS	74
Initial geometric assumptions	75
Idealized geometry	75
Design of the floor system	75
Upper lateral bracing	76
Rib and tie analysis	76
Hanger analysis	80
Computer analysis for live load	80
Minimization of dead load moment	81
Final dead load analysis	81
Final stress analysis and deflection check	81
VI. DESIGN EXAMPLE	83
Problem	83
Solution	83
Hanger tension adjustment	114
SUMMARY	117
BIBLIOGRAPHY	120
APPENDIX	128

LIST OF TABLES

		Page
1.	Parameters of various tied arch bridges.....	37
2.	Cases considered for parametric study of tied arch behavior.....	39
3.	Locations of maximum rib and tie live load moment....	43
4.	Hangers carrying maximum force due to live load.....	59
5.	Computer results for locations of zero rib and tie moment.....	70
6.	Proportion of live load moment carried by the rib and by the tie, for H/L = 1/5.9 cases. Comparison of computer results with results using Equations (27) and (28).....	72
7.	Proportion of live load moment carried by the rib and by the tie, for H/L = 1/5.0 cases. Comparison of computer results with results using Equations (27) and (28).....	73
8.	Values of coefficient ζ.....	79
9.	Rib and tie profile coordinates.....	84
10.	Rib member geometry.....	85
11.	Lengths and weights of upper lateral bracing members.....	95
12.	Summary of preliminary rib member sizes.....	100
13.	Rib and tie maximum negative live load moment distribution.....	101
14.	Rib and tie maximum positive live load moment distribution.....	102
15.	Summary of preliminary tie member sizes.....	104
16.	y Coordinates of rib profile.....	110
17.	Hanger tensions under dead load.....	111

LIST OF TABLES -- Continued

		Page
18.	Member end actions for eliminating hanger stretch....	113
19.	Member end actions used for developing the influence coefficient matrix.....	116
20.	Computer results for maximum positive live load moment.....	129
21.	Computer results for maximum negative live load moment.....	130
22.	Computer results for maximum axial force.....	131
23.	Computer results for preliminary dead load analysis..	132
24.	Computer results for dead load analysis of rib - unmodified geometry.....	133
25.	Computer results for dead load analysis of rib - modified geometry.....	134
26.	Computer results for dead load analysis of rib - modified geometry. Axial shortening effects eliminated.....	135
27.	Computer results for dead load analysis of tie. Axial lengthening effects eliminated.....	136
28.	Computer results for final dead load analysis of entire arch - modified geometry. Axial deformation effects eliminated.....	137
29.	Computer results for maximum arch deflection. Half-span loading with concentrated load at quarter point.....	139
30.	One half of the influence coefficient matrix for an adjustment analysis.....	140
31.	Required cable length adjustments.....	141
32.	Computer results for checking adjustment analysis....	142

LIST OF FIGURES

		Page
1.	Tied arch bridge nomenclature.....	2
2.	Typical modern steel tied arch bridge.....	5
3.	Simply supported beam and corresponding moment diagram.....	8
4.	Shaping beam to match funicular polygon.....	8
5.	Basic tied arch action.....	9
6.	Cambering arch to eliminate dead load deflection.....	10
7.	Solving for horizontal force for parabolically shaped beam.....	12
8.	Tie carrying uniform loading.....	13
9.	Tie carrying non-uniform loading.....	14
10.	Dead load moment diagram for a tied arch.....	16
11.	Solving for horizontal force for parabolically shaped arch.....	17
12.	Mathematical model of rib for computer analysis.....	19
13.	Mathematical model of tie for computer analysis.....	20
14.	Application of a horizontal force to a tightly stretched cable.....	24
15.	Fundamental mode of vibration of a tightly stretched cable.....	26
16.	Cable and hanger numbering conventions for adjustment analysis.....	29
17.	Mobile Arch Bridge geometry.....	40

LIST OF FIGURES -- Continued

		Page
18.	Graph of rib moment influence lines. A_R/A_T = 0.6 ; I_R/I_T = 1/20 ; 16 Panels.....	45
19.	Graph of tie moment influence lines. A_R/A_T = 0.6 ; I_R/I_T = 1/20 ; 16 Panels.....	46
20.	Graph of rib moment influence lines. A_R/A_T = 1.0 ; I_R/I_T = 1.0 ; 16 Panels.....	47
21.	Graph of tie moment influence lines. A_R/A_T = 1.0 ; I_R/I_T = 1.0 ; 16 Panels.....	48
22.	Graph of rib moment influence lines. A_R/A_T = 1.5 ; I_R/I_T = 20 ; 16 Panels.....	49
23.	Graph of tie moment influence lines. A_R/A_T = 1.5 ; I_R/I_T = 20 ; 16 Panels.....	50
24.	Graph of rib moment influence lines. A_R/A_T = 1.0 ; I_R/I_T = 1/10 ; 10 Panels.....	51
25.	Graph of tie moment influence lines. A_R/A_T = 1.0 ; I_R/I_T = 1/10 ; 10 Panels.....	52
26.	Graph of rib moment influence lines. A_R/A_T = 1.0 ; I_R/I_T = 1/10 ; 12 Panels.....	53
27.	Graph of tie moment influence lines. A_R/A_T = 1.0 ; I_R/I_T = 1/10 ; 12 Panels.....	54
28.	Graph of rib moment influence lines. A_R/A_T = 1.0 ; I_R/I_T = 1/10 ; 20 Panels.....	55
29.	Graph of tie moment influence lines. A_R/A_T = 1.0 ; I_R/I_T = 1/10 ; 20 Panels.....	56
30.	Graph of rib moment influence lines. A_R/A_T = 1.0 ; I_R/I_T = 1/10 ; 24 Panels.....	57
31.	Graph of tie moment influence lines. A_R/A_T = 1.0 ; I_R/I_T = 1/10 ; 24 Panels.....	58
32.	Graph showing effect of I_R/I_T ratio upon hanger forces.....	62
33.	Graph showing effect of hanger spacing upon hanger forces.....	63

LIST OF FIGURES -- Continued

		Page
34.	Graph of rib deflection for various cases.....	66
35.	Graph of tie deflection for various cases.....	67
36.	Live load moment in a tied arch.....	69
37.	Assumed geometry of arch.....	86
38.	Cross section of floor.....	87
39.	Plan of lateral floor bracing.....	89
40.	Plan of upper lateral bracing.....	93
41.	Dead load of arch.....	108

ABSTRACT

Preliminary design of a tied arch bridge is complex due to the many possible parameters of the problem. After obtaining a design the minimization of dead load moment is an important consideration. Similarly, obtaining proper tensions in the hangers of a tied arch bridge is very important, to prevent overstressing of the arch.

By using matrix structural analysis, the effects of certain parameters upon tied arch behavior are investigated. The parameters include rise to span ratio, hanger spacing, ratio of areas of rib and tie, and ratio of moments of inertia of rib and tie. The geometry of an existing span was used for analysis.

The results of the parametric study are portrayed graphically for a range of the parameters. Methods for analysis of dead load moment and hanger tension adjustment are developed. Finally a preliminary design example is considered.

CHAPTER I

INTRODUCTION

Description

Tied arch bridges are distinguished from other forms of arch bridges by the presence of a tie chord. Figure 1 shows a typical profile of a tied arch bridge and gives the nomenclature of the parts of the structure. Tied arch behavior is similar to that of a self-anchored suspension bridge. In both cases the effects of live load structural distortion are practically eliminated. The tie girder carries the thrust of the arch rib. Hence, tied arches are ideally suited for sites where foundation conditions will not permit an economical substructure, which could carry the thrust of a conventional arch. Tied arches are also used where moderate span lengths are required with a maximum clearance.

History

The history of the tied or bowstring arch in America can be traced back to Trees' and King's truss, [3]. Trees' and King's truss consisted of tubular iron arches, with a tie beam attached to each end of the arch which supported the roadway. The patent on Trees' and King's truss expired Oct. 1, 1878. Some of the trusses designed by Squire Whipple in the mid-nineteenth century also possessed some

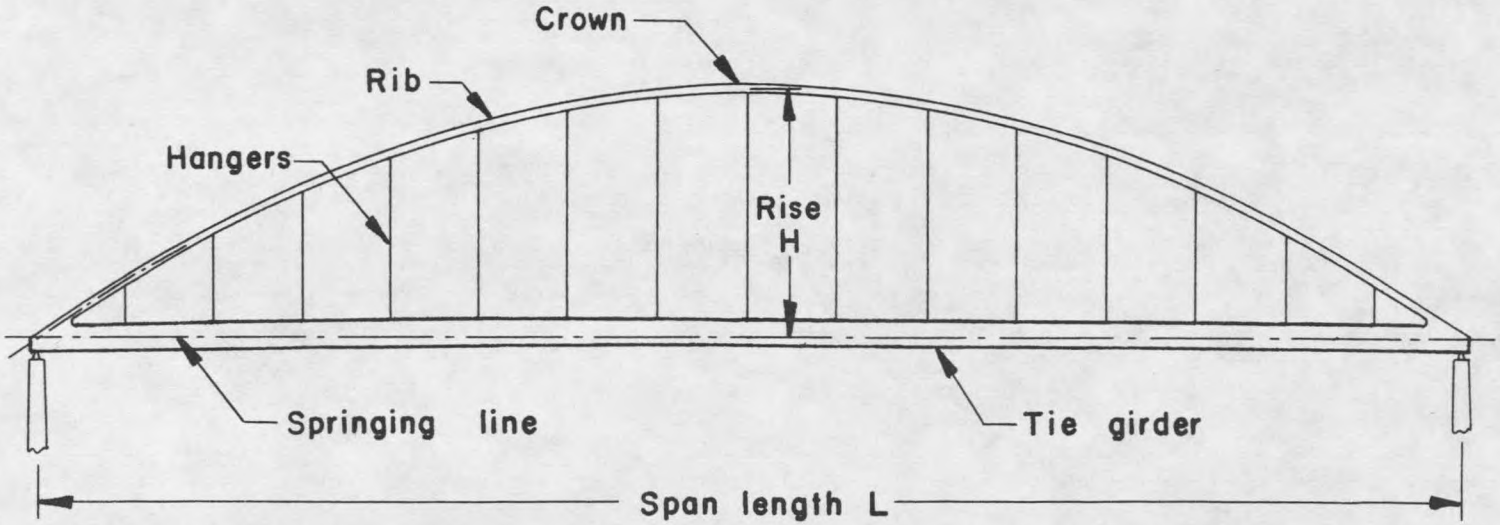

Figure 1. Tied arch bridge nomenclature.

of the features of tied arch construction. The tied arch was also being widely used in the mid-nineteenth century in Europe. The first bowstring arch was at Lugao in Hungary, designed by Hoffman and Medersbach in 1833, [48]. Austrian engineer Joseph Langer designed a truss-tied arch in 1859, [61].

Originally tied arch bridges such as the Tacony-Palmyra [55] or the West End [57] were designed with deep ribs, to carry the majority of the live load moment. In 1941, J. M. Garrelts revolutionized the design of tied arch bridges in America, with the design of the St. Georges Bridge. In the St. Georges Bridge the tie was made about 13 times as stiff as the rib, and therefore carried the majority of the live load moment, [7, 36].

Virtually all tied arch spans constructed today utilize the stiff tie and slender rib concept. In addition to superior aesthetics Garrelts gave the following advantages for this type of tied arch, [7]:

1. The erection will generally require less falsework because the tie girders will support erection equipment over longer spans.

2. The demands on erection equipment are reduced by reason of the fact that the heaviest members are lifted only to the level of the deck rather than to the top of the span. This may in some designs eliminate the necessity of special creeper travelers moving along the rib and permit the use of more common equipment operating from the deck.

3. Although no direct comparison in weight has been made as yet, it can be pointed out that some economy may result from the shorter length of the heavy tie as compared to the longer length of a heavy rib. This saving is partly offset by heavier splices.

4. Since the tie girder will always have little, if any, compression, the ends of the members at splice points need

not be milled. All milling of the splices in the curved rib is therefore confined to lighter, smaller members.

5. The connections at the ends of the span appear to be simplified when the deep girders are horizontal or nearly so, and the transfer of the vertical shear into the shoes is readily accomplished by detail parts that are easier to fabricate. The erection in this panel is much less difficult because a milled splice for the first rib member can generally be located above the tie girder so that the first section of the rib can be erected after the girder has been placed on the shoe and the first hanger erected. No temporary support for a heavy, inclined section of rib is required.

Figure 2 shows a sketch of a typical modern steel tied arch bridge, utilizing a stiff tie and slender rib.

In the 1950's design of tied arches underwent further refinements and improvements. The advent of high strength steels made tied arches competitive economically for much longer spans and heavier loads. Additionally the development of the digital computer led to a much better understanding of tied arch behavior. The Fort Pitt Bridge and Fort Duquesne Bridge in Pittsburgh are two notable double deck tied arch structures constructed in 1957, and 1960 respectively, [63, 65].

By using an orthotropic deck, the dead load of a bridge can be greatly reduced. Two notable tied arch bridges utilizing orthotropic decks are the Port Mann Bridge in 1963, [11, 15, 41], and the award winning Fremont Bridge in 1973, [14]. The Fremont Bridge is the longest tied arch bridge in history with a 1200 foot main span.

Today the science of tied arch bridges is still expanding. In other countries inclined hangers (Nielsen System) are being used [10, 24, 34, 35]. In some cases the entire deck is being used to act as

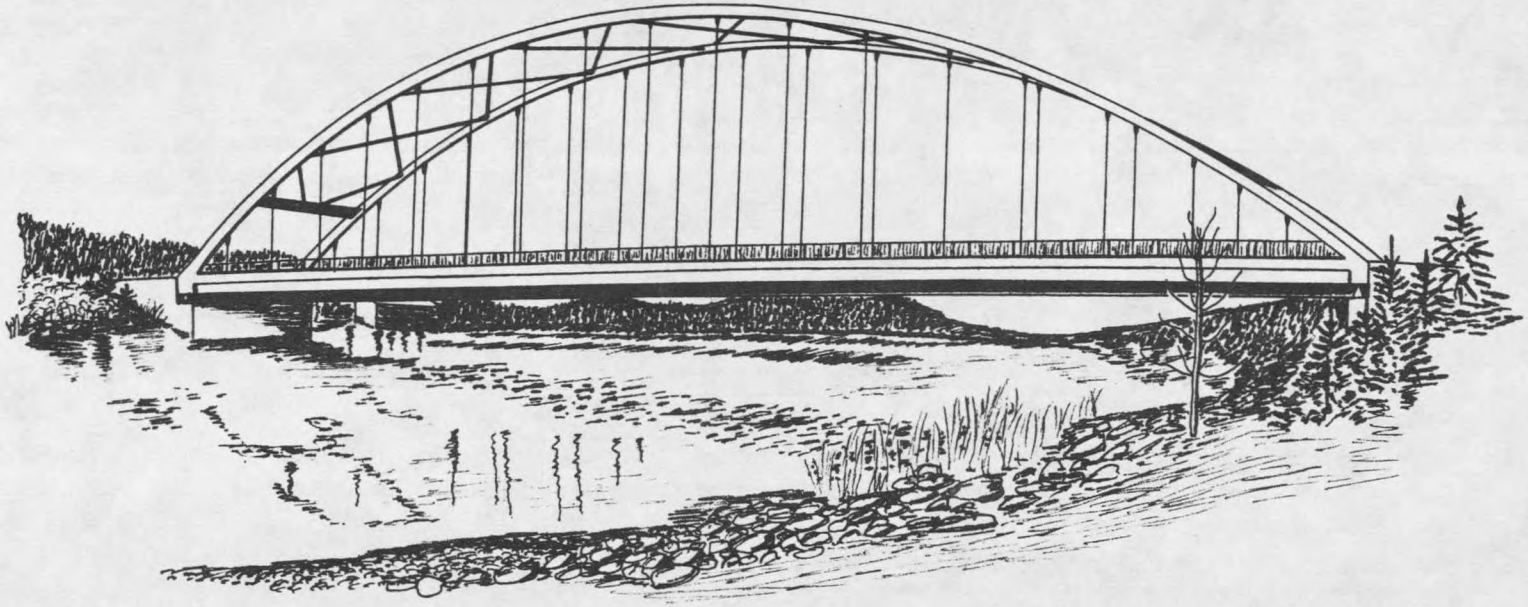

Figure 2. Typical modern steel tied arch bridge.

the tie [48]. For increased stability inclined tied arches are being tried [20, 22, 29]. The use of prestressed concrete for the ribs and for the deck is being investigated [29, 54]. These are all topics which would be of interest for further research and are beyond the scope of this thesis.

CHAPTER II

MINIMIZATION OF DEAD LOAD MOMENTS IN A TIED ARCH

The principle of moment minimization

One of the advantages in the use of an arch is having the ability to eliminate practically all of the dead load moments. To accomplish this the arch axis should be shaped to match the dead load funicular polygon or moment diagram. The moment diagram should be that of an equivalent simply supported beam carrying the dead load of the rib, tie, and the loads of the floor system and upper lateral bracing. If the arch axis is made up of straight members rather than curved members, it is only possible to minimize dead load moments but not totally eliminate them. This is due to the local bending effects between hangers caused by the self weight of the members. Additionally the lengths of the arch members must be fabricated to eliminate dead load deformations.

Application of the principle to a frame example

Figure 3 shows an example of a simple beam loaded with a third point loading and the corresponding moment diagram.

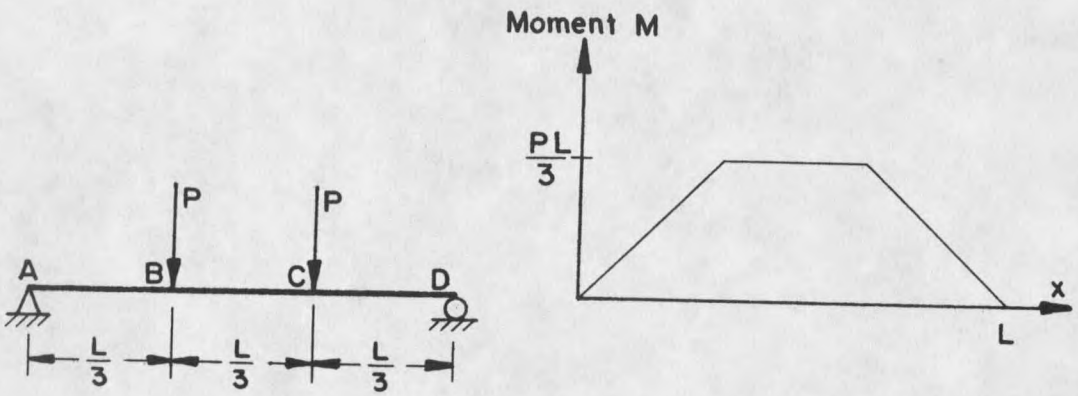

Figure 3. Simply supported beam and corresponding moment diagram.

By reshaping the beam of Figure 3 into a frame corresponding to the moment diagram it can be seen from Figure 4 that the loads P are now being carried primarily axially. There will be secondary moments induced into the frame due to the deformation of the frame.

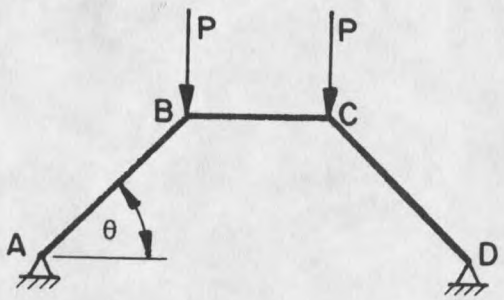

Figure 4. Shaping beam to match funicular polygon.

Also from Figure 4 it can be seen that as the angle θ decreases the axial load in each member increases. Therefore, for an arch, as the rise to span ratio decreases the axial forces in the rib and tie

will increase. Basic tied arch action is accomplished by replacing the rocker at point D of Figure 4 with a roller and adding a tie member AD as shown in Figure 5.

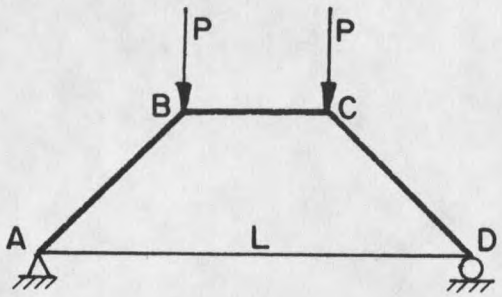

Figure 5. Basic tied arch action.

Under dead load action the arch axis will shorten due to the axial thrust. This effect is called rib shortening. Similarly tie lengthening and hanger stretching will occur due to axial tension. These effects cause secondary moments in the rib and tie which can become quite large. The moments due to rib shortening and tie lengthening can be minimized by fabricating the arch rib longer by a certain amount, and by fabricating the tie shorter by a certain amount. Hangers which are not adjustable also would need to be fabricated shorter by certain amounts. In effect what this does is camber the arch equal and opposite to the deflections induced by the dead load [14], as shown in Figure 6.

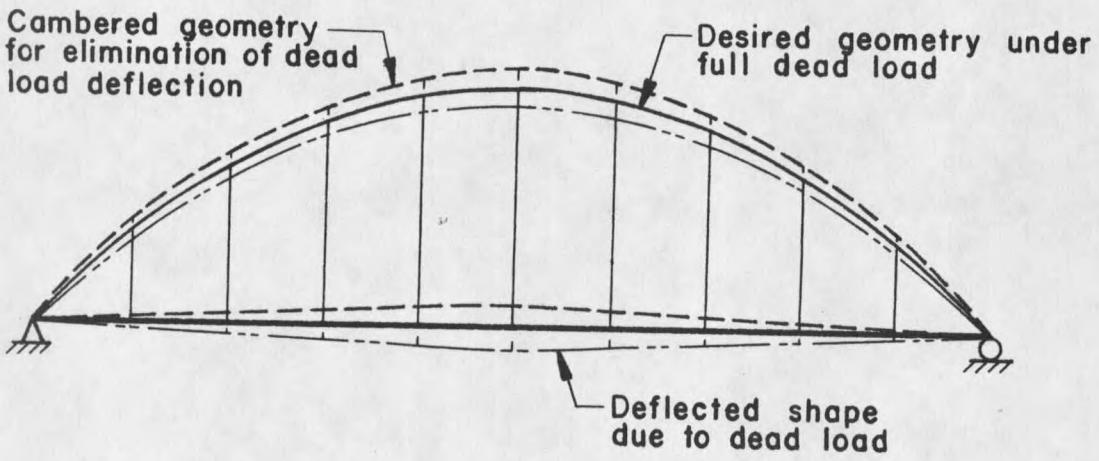

Figure 6. Cambering arch to eliminate dead load deflection.

Referring again to Figure 4 the forces in members AB and CD are found from statics to be P(Cscθ), and for member BC, P(Cosθ). The horizontal thrust at points A and D is also equal to P(Cosθ). The equation for axial deformation in a prismatic member is given by:

$$\delta = \frac{FL}{AE} \qquad (1)$$

where:

δ = Axial deformation
F = Axial force
L = Length of member
A = Area of member
E = Modulus of elasticity

Noting that the lengths of members AB and CD are equal to (Secθ)L/3, the required additional fabricated length to eliminate axial shortening is found from Equation (1) to be:

$$\delta = \frac{P(Csc\theta)(Sec\theta)L}{3AE}$$

Similarly for member BC:

$$\delta = \frac{P(\text{Cos}\theta)L}{3AE}$$

The tie member AD in Figure 5 is required to carry the horizontal thrust, $P(\text{Cos}\theta)$, of members AB and CD. Therefore member AD should be fabricated short by an amount:

$$\delta = \frac{-P(\text{Cos}\theta)L}{AE}$$

In addition to fabricating the members to compensate for changes in length, the geometry of the connections between members must be fabricated to the ideal undeformed shape of the structure. This insures that moments are not induced by angular rotations at the joints due to the changes in lengths of the members. For the frame of Figure 5 this means that angles BAD and CDA would equal θ, and angles ABC and DCB would equal $180° - \theta$.

Application of the principle to a tied arch

The basic ideas presented in the simple frame example can readily be applied to a highly statically indeterminate structure, such as a tied arch. To accomplish this it is convenient to first consider the tie separately, and then consider the entire arch.

For most tied arch bridges the dead load of the floor system including the concrete slab will be nearly uniform across the span. Possible variances in the loading may occur due to different sizes of the lateral floor bracing. Also the cross section of the tie could vary across the span. For a simply supported beam carrying a uniform load the moment diagram is parabolic. Referring to Figure 7, if the

axis of the beam is shaped to a parabola, the moment sum about point B at the centerline yields:

$$Fh + \left(\frac{WL}{2}\right)\frac{L}{4} - \left(\frac{WL}{2}\right)\frac{L}{2} = 0$$

where:

h = Height at centerline
L = Length of span
W = Uniform load per unit length
F = Horizontal force

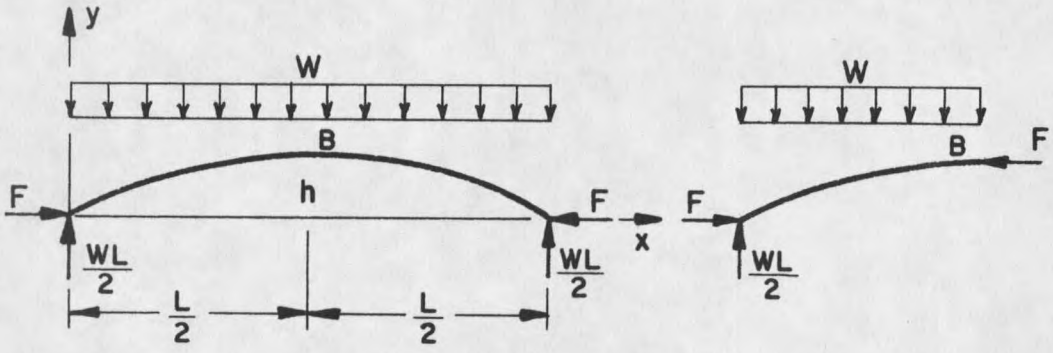

Figure 7. Solving for horizontal force for parabolically shaped beam.

Solving for the horizontal force:

$$F = \frac{WL^2}{8h} \qquad (2)$$

If the floor loads are truly uniform across the span the hanger forces will turn out to all be equal as shown in Figure 8.

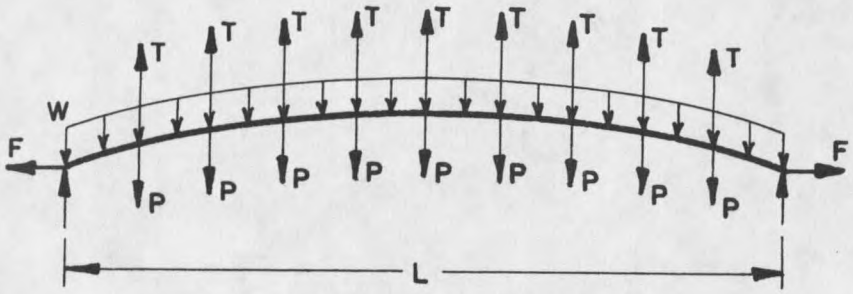

Figure 8. Tie carrying uniform loading.

Noting that the force F in Figure 8 is tensile and opposite in sense to the force F in Figure 7, the net resultant of the the hanger forces T acting upon the tie is an upward uniform loading. Obviously the closer that the hangers are spaced, the more closely a uniform loading is approximated. This means local dead load moments will be smaller.

Referring again to Figure 8, although there are two unknowns F and T, T can be written in terms of F by substitution into Equation (2):

$$F = \left(\frac{T - P}{S} - W \right) \frac{L^2}{8h} \qquad (3)$$

where:

L = Length of tie
T = Hanger tension
F = Horizontal force in tie
W = Weight of tie per unit length
P = Floor system load
S = Distance between hangers
h = Height of tie at centerspan

Equation (3) demonstrates that the tie in itself can be treated as a parabolic arch. For the case of a non-uniform floor loading the net loading can be considered as the sum of a uniform loading P plus a non-uniform loading ΔP_i, as shown in Figure 9.

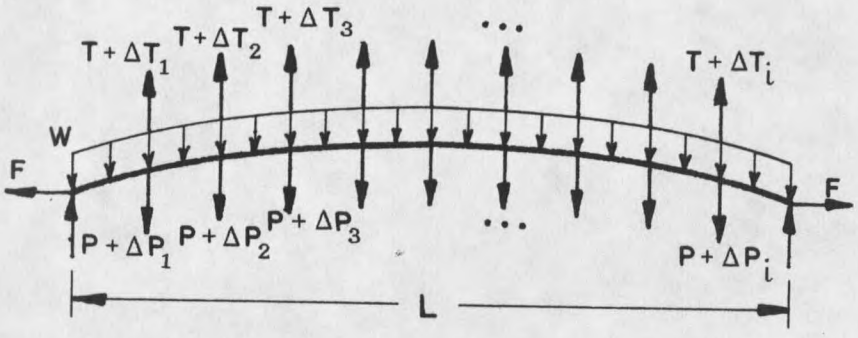

Figure 9. Tie carrying non-uniform loading.

For this case the hanger forces will no longer be equal. From Figure 9 it is apparent however that the non-uniformity of the loading can be directly transmitted into the hangers and carried to the rib. If the weight of the tie varies across the span, the non-uniformity can also be carried into the hangers, although some dead load moment will exist. Therefore the tie can still be modeled as a uniformly loaded parabolic arch.

If the tie is not cambered, the hanger forces will be equal to:

$$T = P + \Delta P_i + WS \qquad (4)$$

where:

T = Hanger tension
P = Floor system load
W = Weight of tie per unit length
S = Distance between hangers

This will not produce the minimum dead load moment, since the geometry of the tie is not conforming to the moment diagram of a similarly loaded simply supported beam. For minimizing the dead load moments in the tie it is probably easiest to shape the tie as a parabola for uniform loading. Any adjustments for non-uniform loading can be made in the geometry of the rib.

The initially assumed geometry of the rib should be checked. If there are no extremely abrupt changes in load across the span, good results can usually be achieved by initially assuming the rib profile to be parabolic. The dead load moment diagram should be constructed for the entire arch. Loads due to the upper lateral bracing and the floor system are treated as concentrated loads applied at the hanger locations. The weights of the rib and tie are treated as distributed loads. A typical shape of a dead load moment diagram for a tied arch is shown in Figure 10.

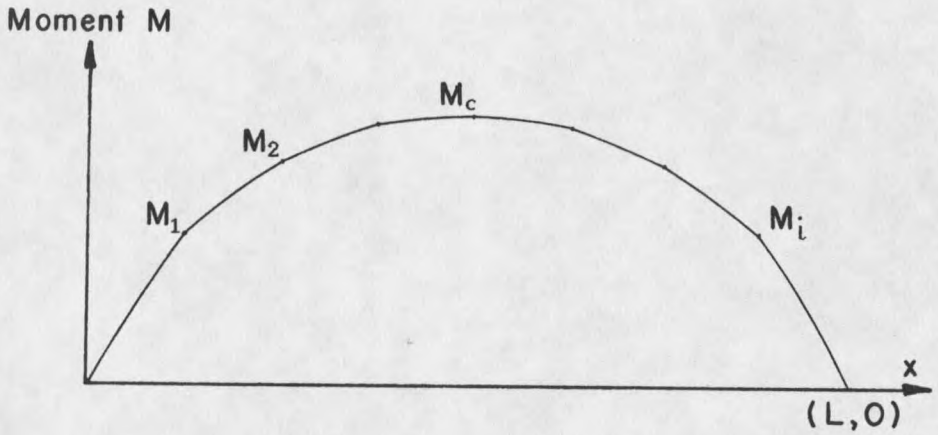

M_i = Internal arch dead load moment at hanger location i
M_c = Internal arch dead load moment at center of bridge

Figure 10. Dead load moment diagram for a tied arch.

The horizontal force F can be determined by equating the internal couple caused by F to the internal dead load moment M_c at the center of the bridge. Referring to Figure 11, and assuming the height H of the rib at the center of the bridge to remain unchanged:

$$F(H-h) = M_c$$

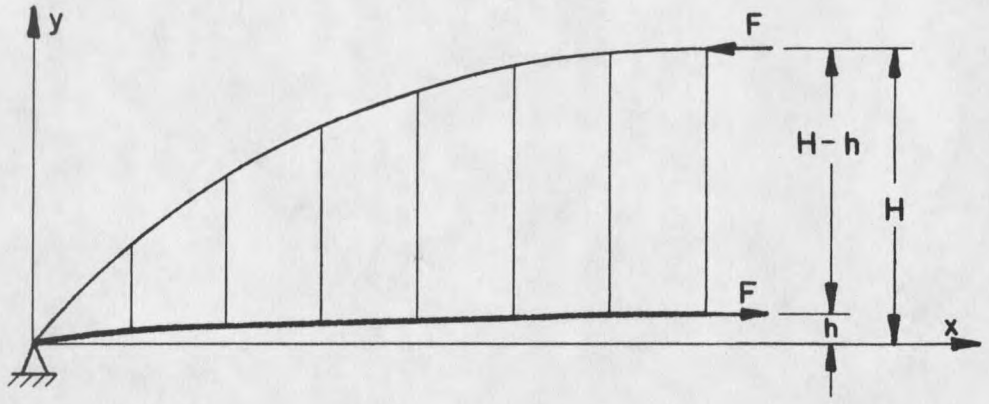

Figure 11. Solving for horizontal force for parabolically shaped arch.

Solving for the horizontal force:

$$F = \frac{M_c}{H - h} \tag{5}$$

Now that the tensile force F in the tie is known, the remainder of the rib geometry can be determined from:

$$H_i = \frac{M_i}{F} + h_i \tag{6}$$

where:

H_i = Ordinates of rib profile
h_i = Ordinates of tie profile (parabolic)
M_i = Internal arch dead load moment at hanger location i

The ordinates of the rib profile should be set equal to the values of H_i. If the values of H_i calculated from Equation (6) differ greatly from the initially assumed values, it may be necessary to recalculate the weights of the rib members based upon the new geometry. The dead load moment diagram would have to be modified accordingly.

The hanger forces can now be determined by eliminating F from Equations (3) and (5), and adding the non-uniform loading ΔP_i:

$$T_i = \frac{8ShM_c}{L^2(H-h)} + P + \Delta P_i \qquad (7)$$

Referring to Figure 9, the value of $P + \Delta P_i$ in Equation (7) represents the total dead load floorbeam reaction at hanger location i.

Computer analysis

The axial loads induced in the rib members can now be determined most readily by computer, considering the ends of the rib as fixed. The forces could also be calculated by dividing the horizontal force F at centerspan by the cosines of the angles of inclination of the rib segments. The loaded rib is shown in Figure 12. The distributed loads would be entered as equivalent member end actions.

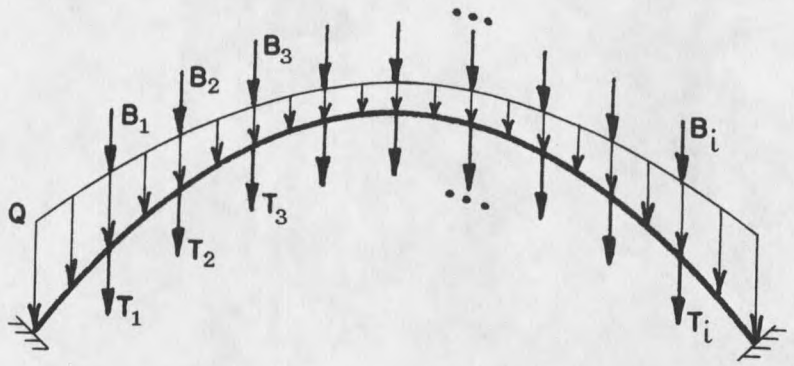

B_i = Weight of upper bracing at hanger location i
T_i = Hanger tension at location i
Q^i = Weight of rib per unit length

Figure 12. Mathematical model of rib for computer analysis.

The axial forces computed in the analysis are now entered into the data as axial member end actions. As mentioned previously the connections must be fabricated to the undeformed geometry. Additionally if the members are curved the radius of curvature must be fabricated to the undeformed shape.

A second computer analysis should show practically zero deflection at all joints and small moments due to local bending between joints. If the axial loads computed in this second analysis are larger than the axial loads input as member end actions from the first analysis, it will be necessary to repeat the process. The axial forces from the second analysis are entered as member end actions and another analysis is made. Convergence to the solution is very rapid,

usually within one or two tries, and occurs when the calculated axial forces equal the input axial member end actions. Substitution of the axial forces into Equation (1) determines the required lengthening adjustments for the rib members.

Although the tension in the tie is already known, an analysis should be made to determine the deflections of the joints. The tie can be modeled as fixed at one end and free to translate in the horizontal direction at the other, as shown in Figure 13.

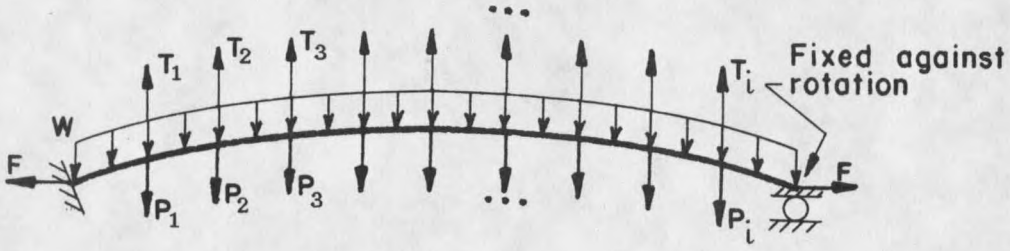

T_i = Hanger tension at location i
P^i = Floor load at hanger location i
W^i = Weight of tie per unit length

Figure 13. Mathematical model of tie for computer analysis.

An analysis is made of the tie similar to the rib analysis including axial member end actions equal to the tensile force F. When calculating the member end actions it may be necessary to adjust the force F to account for the camber in the tie. This is accomplished by:

$$AML = \frac{F}{Cos\theta} \qquad (8)$$

where:

AML = Axial member end action
F = Horizontal force
θ = Angle of inclination of tie segment from horizontal

The final joint deflections are determined and should be very small. Substitution of the axial force in the tie into Equation (1) yields the required shortening adjustments for the tie members.

The required fabrication lengths of the hangers are determined by first computing the relative vertical displacements between the rib and the tie at each hanger location:

$$\delta y_i = \delta y_R - \delta y_T \tag{9}$$

where:

δy_i = Relative vertical displacement between rib and tie of hanger i
δy_R = Vertical displacement of rib joint of hanger i
δy_T = Vertical displacement of tie joint of hanger i

The values of δy_i should be very small if rib shortening effects are properly eliminated. The required shortening adjustments for the hangers are determined from:

$$\delta l_i = - \frac{T_i l_i}{E A} + \delta y_i \tag{10}$$

where:

T_i = Hanger tension at location i
l_i = Length of hanger i
E_i = Modulus of elasticity
A = Area of hanger
δl_i = Length that hanger i is to be fabricated short

The calculation of δy_i and δl_i would not be necessary for adjustable length hangers. In any case it is good to make a final dead load analysis of the entire arch by inputing the computed member end actions for the rib and the tie, and converting the δl_i of Equation (10) to equivalent axial member end actions for the hangers. The final analysis should indeed show that the dead load moments are much smaller than those of a comparable analysis without the geometry changes or the axial deformations taken into account.

CHAPTER III

HANGER TENSION ADJUSTMENT

The structural shapes used for hangers in tied arch bridges generally are box, I or W shapes, or wire rope. Designs using wire rope hangers can be incorporated with provisions for adjusting the tension in the hangers. Typically a threaded strand socket is used at the connection of the hanger and the tie. Designs using solid shaped hangers usually are not provided with means of tension adjustment. Non-adjustable arches require very good quality control during fabrication, to insure that secondary stresses due to misfit are not induced into the arch. Vibration problems have occurred with the use of H shaped hangers, such as the breakage which occurred in the Tacony-Palmyra Bridge, [56].

Arches that are provided with adjustment must be "tuned", sometimes at several phases of the construction. The most convenient times during construction for hanger adjustment are after all steelwork has been erected, and after the deck slab has been completed. Failure to achieve the correct design tensions in the hangers could result in serious overstressing of the rib and tie.

In order to carry out an adjustment analysis the following must be known:

1.) The actual tension in each hanger cable.
2.) The desired tension in each hanger cable.
3.) The relationship between the force induced in cable u due to a unit axial deformation applied to cable v.

The biggest problem in the analysis is determining the actual hanger tensions. Several methods are available for accomplishing this:

1.) Force - deflection method.
2.) Frequency of vibration method.
3.) Strain gages.

Methods of determining hanger tensions

1.) Force-deflection method

By applying a known horizontal force P at a known distance e between two points on a tightly stretched cable, the tension T can be found from static equilibrium. Referring to Figure 14 and equating the sum of horizontal forces to zero yields:

$$-P + T(\text{Sin}\alpha) + T(\text{Sin}\beta) = 0$$

where:

P = Known applied horizontal force
T = Tension in cable

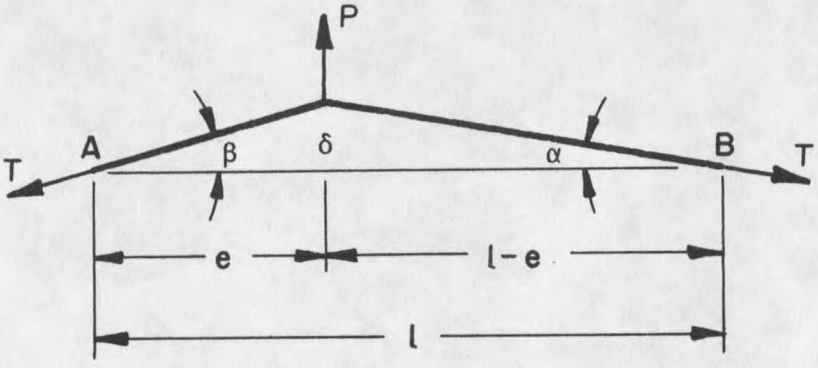

Figure 14. Application of a horizontal force to a tightly stretched cable.

Solving for the tension:

$$T = \frac{P}{\sin\alpha + \sin\beta} \tag{11}$$

The angles α and β can be determined from the relationships:

$$\alpha = \tan^{-1}\left(\frac{\delta}{h-e}\right) \qquad \text{and:} \qquad \beta = \tan^{-1}\left(\frac{\delta}{e}\right)$$

This method is commonly used because of the simplicity and accuracy.

2.) Frequency of vibration method

The tensions in a tightly stretched cable can be determined from measurements of the frequency of vibration and mode shape. Referring to Figure 15 it can be shown that the frequencies of vibration of a tightly stretched cable satisfy the one-dimensional wave equation:

$$\frac{\partial^2 y}{\partial t^2} = a^2 \frac{\partial^2 y}{\partial x^2} \tag{12}$$

where:

T = Tension in cable
g = Acceleration due to gravity
w = Weight per unit length of cable
l = Length of cable

and: $a^2 = \frac{Tg}{w}$

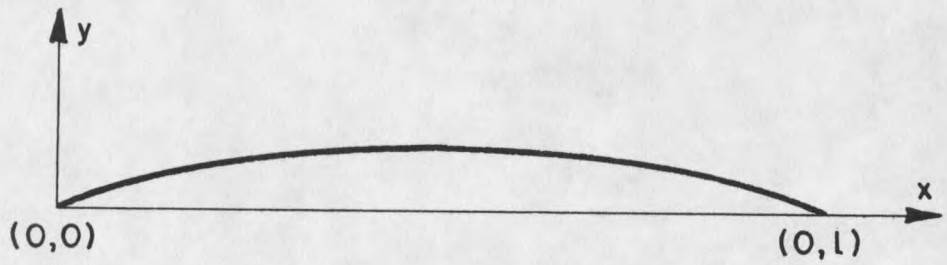

Figure 15. Fundamental mode of vibration of a tightly stretched cable.

After trying a solution of the form $y(x,t) = \chi(x)\tau(t)$ which employs separation of variables, substitution into Equation (12) yields:

$$\frac{\tau''}{\tau} = a^2 \frac{\chi''}{\chi} = \mu \quad (\mu \text{ constant}) \tag{13}$$

The general solution of Equation (13) is found to be:

$$y(x,t) = (A \cos \lambda t + B \sin \lambda t)(C \cos \frac{\lambda x}{a} + D \sin \frac{\lambda x}{a}) \tag{14}$$

$$\text{for } \mu = \lambda^2 \quad \text{and} \quad \lambda < 0$$

This is a periodic function repeating itself each time t increases by $2\pi/\lambda$. Therefore the frequency of vibration is given by:

$$f = \frac{\lambda}{2\pi} \tag{15}$$

Noting in Equation (14) that the solution A = B = 0 produces no motion, this solution is rejected as a trivial solution. The boundary conditions are seen to be $y(0,t) = 0$ and $y(1,t) = 0$. Substitution of the boundary conditions into Equation (14) yields C = 0. Eliminating

the possibility D = 0 as another trivial solution the following is obtained:

$$\text{Sin}\left(\frac{\lambda l}{a}\right) = 0 \quad \text{or:} \quad \frac{\lambda_K l}{a} = K\pi, \; K = 1, 2, 3, \ldots$$

Solving for λ_K and substituting into Equation (15) yields:

$$f_K = \frac{aK}{2l}$$

Therefore the expression for the natural frequencies of vibration of a tightly stretched cable is given by:

$$f_K = \frac{K}{2l}\sqrt{\frac{Tg}{w}} \tag{16}$$

where:

f_K = Frequency for the Kth mode
K^K = Mode of vibration

To determine the tension, the hanger is vibrated and the number of cycles per unit time is measured either visually or electronically. The mode shape must be visually determined.

3.) Strain gages

Strain gages could also be utilized for determining hanger tensions. The cost of this method would probably be greater than that of other methods. It would be important to attach a strain gage to a hanger before any stress is induced into the hanger. After placing the hanger in the arch the tension can be determined directly, by reading the value from a strain indicator. By using a multi-channel strain indicator it would be possible to monitor the strains in all

hangers simultaneously. This would be advantageous during the adjustment process.

Analysis

The preliminary step for the adjustment analysis is determining the actual tension in each hanger. For hangers with multiple cables the tension in each individual cable must be determined as they probably will not be equal. The analysis can be carried out most readily using matrix structural analysis on a computer. Most tied arch bridges can be modeled as if each arch behaves as a planar frame. Therefore no interaction occurs between arches due to the floor beams or the upper lateral bracing. If there is interaction between arches a space frame analysis can be used. Figure 16 shows the assumed hanger and cable numbering conventions. The analysis is written assuming four cables per hanger, giving a total of 4i cables per arch. The procedure applies for any number of cables however.

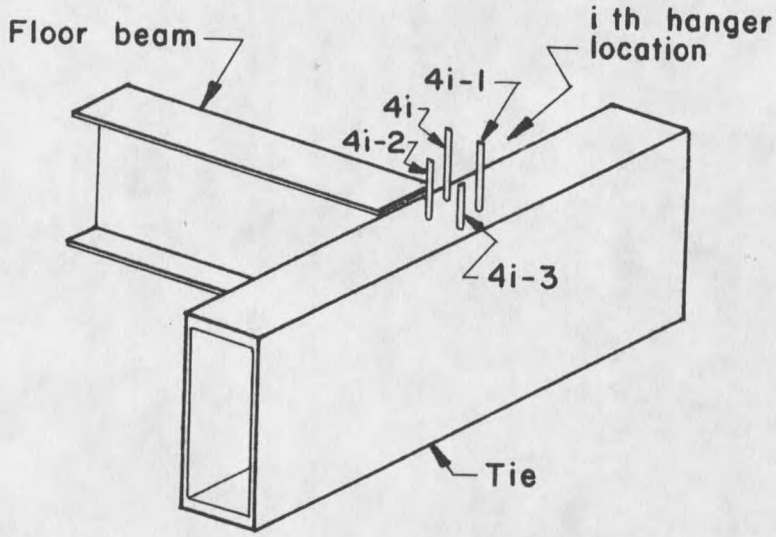

Cable Numbers

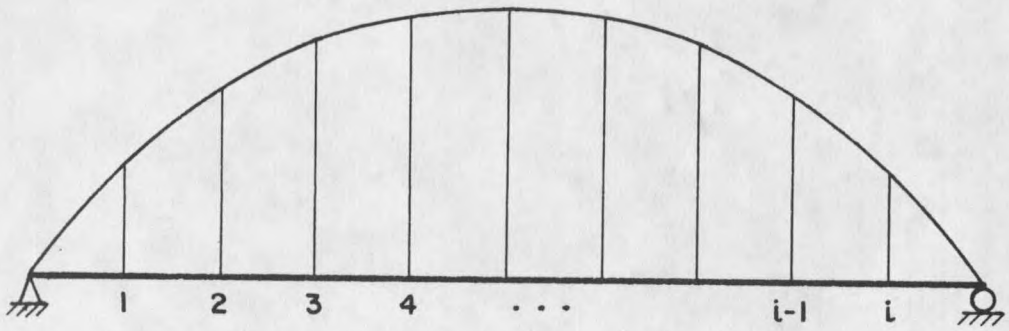

Hanger Numbers

Figure 16. Cable and hanger numbering conventions for adjustment analysis.

The required tension adjustments $\{\Delta T\}$ for all cables are obtained from the relationship:

$$\{\Delta T_u\} = \{T_u\} - \{I_u\} \quad \text{for } u = 1,4i \tag{17}$$

where:

$\{\Delta T_u\}$ = Required tension adjustments
$\{T_u\}$ = Final desired tensions
$\{I_u\}$ = Actual cable tensions

Starting with cable 1 at hanger location 1 it is necessary to develop an influence coefficient matrix $[K_{uv}]$. The matrix relates the force induced in cable u due to a unit axial deformation applied to cable v. The matrix $[K_{uv}]$ therefore has the dimension 4i by 4i. Using this influence coefficient matrix the required tension adjustments $\{\Delta T\}$ can be related to the required length adjustments $\{D\}$ by the equation:

$$[K_{uv}]\{D_u\} = \{\Delta T_u\} \quad \text{for } u = 1,4i \; ; \; v = 1,4i \tag{18}$$

After partitioning the matrix $[K_{uv}]$ in terms of hanger locations, Equation (18) can be rewritten:

$$[k_{mn}]\{d_m\} = \{\Delta t_m\} \quad \text{for } m = 1,i \; ; \; n = 1,i \tag{19}$$

In expanded notation:

$$\begin{bmatrix} k_{11} & k_{12} & k_{13} & \cdots & k_{1n} & \cdots & k_{1i} \\ k_{21} & k_{22} & k_{23} & \cdots & k_{2n} & \cdots & k_{2i} \\ k_{31} & k_{32} & k_{33} & \cdots & k_{3n} & \cdots & k_{3i} \\ \vdots & \vdots & \vdots & & \vdots & & \vdots \\ k_{m1} & k_{m2} & k_{m3} & \cdots & k_{mn} & \cdots & k_{mi} \\ \vdots & \vdots & \vdots & & \vdots & & \vdots \\ k_{i1} & k_{i2} & k_{i3} & \cdots & k_{in} & \cdots & k_{ii} \end{bmatrix} \begin{Bmatrix} d_1 \\ d_2 \\ d_3 \\ \vdots \\ d_m \\ \vdots \\ d_i \end{Bmatrix} = \begin{Bmatrix} \Delta t_1 \\ \Delta t_2 \\ \Delta t_3 \\ \vdots \\ \Delta t_m \\ \vdots \\ \Delta t_i \end{Bmatrix}$$

where:

$$[k_{mn}] = \begin{bmatrix} K_{4m-3,\ 4n-3} & K_{4m-3,\ 4n-2} & K_{4m-3,\ 4n-1} & K_{4m-3,\ 4n} \\ K_{4m-2,\ 4n-3} & K_{4m-2,\ 4n-2} & K_{4m-2,\ 4n-1} & K_{4m-2,\ 4n} \\ K_{4m-1,\ 4n-3} & K_{4m-1,\ 4n-2} & K_{4m-1,\ 4n-1} & K_{4m-1,\ 4n} \\ K_{4m,\ 4n-3} & K_{4m,\ 4n-2} & K_{4m,\ 4n-1} & K_{4m,\ 4n} \end{bmatrix}$$

$$\{d_m\} = \begin{Bmatrix} D_{4m-3} \\ D_{4m-2} \\ D_{4m-1} \\ D_{4m} \end{Bmatrix} \qquad \text{and:} \quad \{\Delta t_m\} = \begin{Bmatrix} \Delta T_{4m-3} \\ \Delta T_{4m-2} \\ \Delta T_{4m-1} \\ \Delta T_{4m} \end{Bmatrix}$$

Assuming that the connections between the hangers and the rib and tie are very stiff the deflection due to bending of the connections can be neglected. Therefore all cables of a hanger deflect equally. With this assumption the influence coefficients relating the cables 4m, 4m-1, 4m-2, and 4m-3, at a particular hanger m can be written:

$$K_{4m-3,\ 4m-3} = K_{4m-2,\ 4m-2} = K_{4m-1,\ 4m-1} = K_{4m,\ 4m} = AML - S_{mm} \qquad (20i)$$

and:

$$K_{4m-3,\ 4m-2} = K_{4m-3,\ 4m-1} = K_{4m-3,\ 4m} = -S_{mm} \qquad (20ii)$$

$$K_{4m-2,\ 4m-3} = K_{4m-2,\ 4m-1} = K_{4m-2,\ 4m} = -S_{mm} \qquad (20iii)$$

$$K_{4m-1,\ 4m-3} = K_{4m-1,\ 4m-2} = K_{4m-1,\ 4m} = -S_{mm} \qquad (20iv)$$

$$K_{4m,\ 4m-3} = K_{4m,\ 4m-2} = K_{4m,\ 4m-1} = -S_{mm} \qquad (20v)$$

where:

S_{mm} = Force induced in three cables at hanger location m due to application of a unit deformation to the forth cable at hanger location m.

AML = Force required to produce unit deformation in the forth cable.

In Equations (20) and (21) S_{mm} is assumed to be positive to produce positive tensile forces. Substituting (20i) - (20v) into the expression for $[k_{mn}]$ in Equation (19), and noting that m = n, the following is obtained:

$$[k_{mm}] = S_{mm}\begin{bmatrix} \frac{AML - S_{mm}}{S_{mm}} & -1 & -1 & -1 \\ -1 & \frac{AML - S_{mm}}{S_{mm}} & -1 & -1 \\ -1 & -1 & \frac{AML - S_{mm}}{S_{mm}} & -1 \\ -1 & -1 & -1 & \frac{AML - S_{mm}}{S_{mm}} \end{bmatrix} \quad \text{for } m = n \qquad (21)$$

Similarly, the forces induced in the four cables at hanger location m due to the unit deformation of a cable at location n will be equal. This can be expressed as:

$$[k_{mn}] = S_{mn}\begin{bmatrix} 1 & 1 & 1 & 1 \\ 1 & 1 & 1 & 1 \\ 1 & 1 & 1 & 1 \\ 1 & 1 & 1 & 1 \end{bmatrix} \qquad \text{for } m \neq n \quad (22)$$

where:

S_{mn} = Force induced in a cable at hanger location m due to application of a unit deformation to a cable at hanger location n.

The coefficient S_{mn} in Equation (22) is assumed positive to produce positive tensile forces. When applying the unit deformation to a cable for calculating S_{mm} and S_{mn}, it is usually more convenient to convert to an equivalent member end action:

$$AML = \frac{AE}{l} \qquad (23)$$

where:

AML = Equivalent member end action
A = Area of cable
E = Modulus of elasticity
l = Length of cable

The remaining three cables at the hanger being loaded can be combined into a single equivalent member. Similarly the four cables at all other hangers can be combined into single equivalent members.

Since the arch geometry is symmetric, S_{mm} and S_{mn} only have to be calculated for half of the hangers.

With the formation of the $[K_{uv}]$ matrix, the required length adjustments to be made to the hangers are solved for from Equation (18):

$$\{D_u\} = [K_{uv}]^{-1} \{\Delta T_u\} \tag{24}$$

The length adjustments $\{D_u\}$ can also be written in terms of the required turns of the adjusting nuts:

$$\{N_u\} = \{D_u\}(p) \tag{25}$$

where:

$\{N_u\}$ = Required turns of the adjusting nuts
$\{D_u\}$ = Required length adjustments
p = Pitch of the thread (turns/length)

When performing the adjustment to the bridge, hangers should be alternately tightened on each side of the arch. This should minimize the possibility of overstressing the rib or tie during adjustment. If any hanger tensions vary excessively from the design values, it may be necessary to compute the stresses in the arch. Since this is a closed form solution the tightening sequence will not affect the final results. There is the distinct possibility however of overstressing the rib or the tie during adjustment. This may have to be checked.

CHAPTER IV

EFFECTS OF VARIOUS PARAMETERS UPON TIED ARCH BEHAVIOR

Discussion of parameters

Preliminary analysis of a tied arch is complex due to the many possible geometric and member parameters for a structure. The effects of some of the various parameters on the behavior of a tied arch were investigated. The parameters considered in this discussion are:

1.) Rise to span ratio.
2.) Ratio of moments of inertia of rib and tie.
3.) Ratio of areas of rib and tie.
4.) Hanger spacing.

Other important design parameters which must be considered include:

1.) Type of rib, tie, and deck.
2.) Type of joint at connection of rib and tie.
3.) Tie depth to span ratio.
4.) Rib depth to span ratio.
5.) Curved rib versus segmental rib.

Tied arches can be designed within a wide range of the various parameters. The question of economics must be considered in conjunction with design efficiency. For example, structurally it is desirable to space the hangers as close as possible. Economically this is not feasible, even though the dead load of the structure will decrease. Similarly if the hanger spacing becomes too large the savings in materials and labor will be more than offset by the cost of the increased dead load. Again this makes an uneconomic alternative.

Therefore when choosing the hanger spacing, the cost of installing a hanger must be considered along with the cost per foot of floor system and rib.

Aesthetics also form a very important part of the selection of parameters. An arch which uses straight segments between panel points may not have a pleasing appearance if the hangers are spaced too far apart. This would produce sharp angular changes at the panel points and break the continuity of the rib. Aesthetics can also enter into the consideration of rib and tie depths. Many times a certain tie depth is determined which will correspond with the girder depths of the approach spans.

Table 1 gives some values of the typical parameters used for various bridges with span lengths ranging from 116 feet to 1200 feet. Richardson [37] compiled photos and overall dimensions of various arch bridges, and is an excellent source of information for preliminary designs. The parameter ranges found from Table 1 primarily of interest for this study are:

1. Arch rise to span ratio typically lies within 1/5 and 1/6.5.
2. For arches with deep ties and shallow ribs, tie depth to span ratio typically lies within 1/50 and 1/70.
3. Ratio of moments of inertia of rib to tie for solid rib and tie bridges typically lies within 1/20 and 25/1.
4. Ratio of span to hanger spacing typically lies within 10 and 20.
5. Ratio of areas of rib to tie for solid rib and tie bridges typically lies within 0.6 and 1.5.

Table 1[1]. Parameters of various tied arch bridges.

Name of Bridge Route No. / River Spanned Location / Date Constructed	No. of Lanes	Type of Tie	Type of Rib	Length	Rise	$\frac{L}{H}$	No. of Panels	Rib Crown Depth	Tie Center Depth	$\frac{\text{Length}}{\text{Tie Depth}}$	$\frac{A_R}{A_T}$	$\frac{I_R}{I_T}$	Hangers	Notes
Old Mill Road Old Mill Road, Chagrin Cleveland, OH, 1959	2	I	Channel	116.0'	25.0'	4.64	7	1.5'	3.0'	38.67	0.64^{2}	0.13^{2}	12WF31	
North Fork Stillaguamish U.S. 410, N.Fork Stillaguamish Cicero & Snohomish Co.,WA,1966	2	Box	Box	278.7'	51.0'	5.50	11	2.0'	4.0'	69.67	0.81^{2}	0.22^{2}	8x8x3/8 Tubing	
Bonar A9 Highway, Dornoch Firth Scotland, 1975	2	I	Box	341.5'	61.4'	5.56	17	2.3'	5.6'	61.20	1.08^{3}	0.17^{3}	64mm Coil Cable	
Leavenworth Centennial Missouri River Leavenworth, KA, 1955	2	Box	Box	420.0'	80.0'	5.25	13	2.8'	6.2'	67.74	0.74^{2}	0.15^{2}	HP12x53	Two Arches
Fort Duquesne Allegheny River Pittsburgh, PA, 1960	8	Truss	Box	423.0'	$64.6'^{6}$	6.55	9	4.0'	23.5'	18.00	0.95^{7}	0.02^{7}	2-3/4" Wire Rope	Double Deck
St. Georges, Dupont Hwy. Chesapeake & Delaware Canal St. Georges, DE, 1940	4	Box	Channel	539.4'	104.1'	5.18	15	3.4'	9.0'	59.93	0.73^{3}	0.08^{3}	Box	
Fort Henry Ohio River Wheeling, WVa, 1955	4	Plates	Box	577.5'	110.9'	5.20	15	9.2'	2.8'	204.1	1.46^{2}	26.7^{2}	W14x103	
LaSalle - Peru Route 412, Illinois River LaSalle, IL, 1984	4	I	Box	620.5'	123.6'	5.00	17	4.0'	11.0'	56.41	0.82^{2}	0.12^{2}	1-5/8" Wire Rope	

Table 1[1] Continued. Parameters of various tied arch bridges.

Name of Bridge Route No. / River Spanned Location / Date Constructed	No. of Lanes	Type of Tie	Type of Rib	Length	Rise	$\frac{L}{H}$	No. of Panels	Rib Crown Depth	Tie Center Depth	$\frac{\text{Length}}{\text{Tie Depth}}$	$\frac{A_R}{A_T}$	$\frac{I_R}{I_T}$	Hangers	Notes
Fort Pitt Monongahela River Pittsburgh, PA, 1957	8	Truss	Box	750.0'	122.2'[6]	6.14	15	5.4'	24.9'	30.10	0.94[5]	0.04[5]	3-1/4" Wire Rope	Double Deck
Glenfield I - 79, Ohio River Neville Island, PA, 1974	6	Box	Box	750.0'	124.4'	6.03	15	4.0'	12.5'	60.00	0.64[2]	0.06[2]	2-7/8" Wire Rope	
West End Ohio River Pittsburgh, PA, 1932	4	Plates	Truss	778.0'	151.0'[4]	5.15	28	25.0'	3.3'	233.6	1.21[2]	183[2]	4" Wire Rope	Truss Arch Rib
Sherman Minton I - 64, Ohio River Louisville, KY, 1961	6	Box	Truss	797.5'	140.0'[4]	5.70	22	30.0'	3.2'	251.6	1.86[2]	328[2]	2-1/2" Wire Rope	Truss Rib Double Deck
Mobile Arch I - 65, Mobile River Delta Mobile, AL, 1977	2	Box	Box	800.0'	136.0'	5.88	16	4.9'	14.0'	57.14	1.09[2]	0.15[2]	1-5/8" Wire Rope	
Port Mann, Trans-Canada Hwy. Lower Fraser River New Westminster, BC, 1962	4	Box	Box	1200.0'	230.0'	5.22	24	4.4'	12.0'	Half through tied arch with orthotropic deck and 360' sidespans.				
Fremont I - 405, Williamette Portland, OR, 1973	8	Box	Box	1255.3'	448.3'	3.00	28	4.0'	18.0'	Half through tied arch with orthotropic deck and 448' sidespans.				

1. Data collected from Richardson [37] and drawings from various consulting firms.
2. Values taken at center of span.
3. Values taken at 0.20 point of span.
4. From springing line to lower chord of rib truss.
5. Values taken at 0.25 point of span.
6. From top chord of tie truss to rib.
7. Values taken at 0.44 point of span.

To study the effects that the parameters have upon tied arch behavior, the Mobile Arch Bridge, designed by the consulting firm of Howard Needles Tammen & Bergendoff was selected for analysis. The geometry for the Mobile Arch Bridge is given in Figure 17. The cases considered for study are given in Table 2.

Table 2. Cases considered for parametric study of tied arch behavior.

Case No.	$\frac{I_R}{I_T}$	$\frac{A_R}{A_T}$	s
1/20-12	1/20	0.6	12
1/20-16	1/20	0.6	16
1/20-20	1/20	0.6	20
1/10-10	1/10	1.0	10
1/10-12	1/10	1.0	12
1/10-16	1/10	1.0	16
1/10-20	1/10	1.0	20
1/10-24	1/10	1.0	24
1-12	1.0	1.0	12
1-16	1.0	1.0	16
1-20	1.0	1.0	20
20-12	20.0	1.5	12
20-16	20.0	1.5	16
20-20	20.0	1.5	20

where:

$\frac{I_R}{I_T}$ = Ratio of moments of inertia of rib to tie at centerspan

$\frac{A_R}{A_T}$ = Ratio of areas of rib to tie at centerspan

s = Number of panels

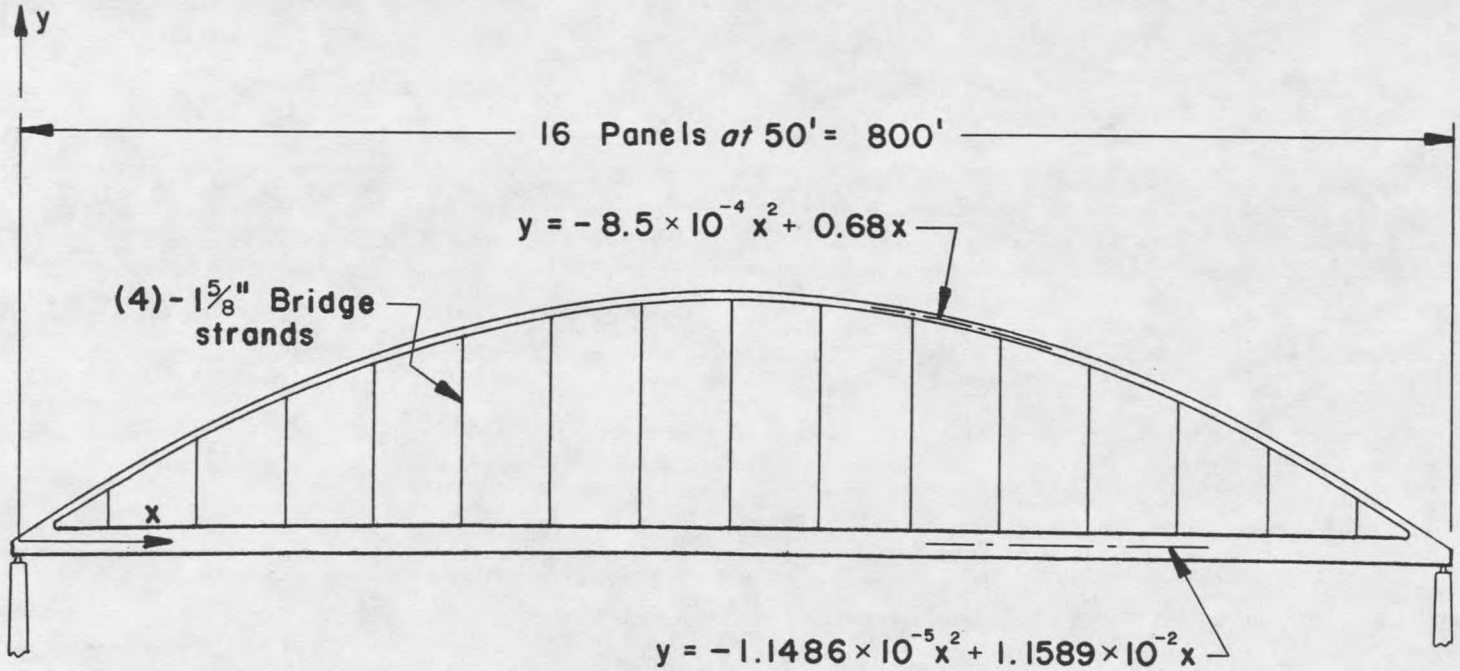

Arch rise at centerspan, H = 136'
Tie rise at centerspan, h = 2.3'

Figure 17. Mobile Arch Bridge geometry.

It was decided to keep the cross sectional area of the arch at centerspan constant at 600 in^2. Similarly the total moment of inertia of the rib plus tie was held constant at 1.5 x 10^6 in^4. The rib and tie areas and moments of inertia were held constant across the span. The hanger area remained constant at 8.3 in^2. All of the cases were run for a rise to span ratio (H/L) of 1/5.9. Some of the cases were repeated for an H/L ratio of 1/5.0.

The analysis was carried out by computer using matrix structural analysis. The member element used in the analysis allowed axial and flexural deformations, and gave a linear first order solution. Therefore axial-flexural interaction was not accounted for. The size effects of the connection at the rib and tie were also neglected.

The results were analyzed in terms of:

1. Rib and tie moment influence lines.
2. Hanger forces.
3. Rib and tie deflection.
4. Proportion of live load moment carried by the rib and by the tie.

Rib and tie moment influence lines

Figures 18 through 23 show the graphs of the rib and tie moment influence lines for three of the 16 panel cases. The H/L ratio for all cases is 1/5.9. The curves look similar to those predicted by Garrelts [7].

In all cases the rib moment influence lines tend to be more rounded near the peaks. This indicates distribution of moment to adjacent panels, as the rib deforms. The tie moment influence lines show much sharper peaks, especially when I_R/I_T becomes large. This

indicates more localized bending at the point of load application. All curves indicate the same shape of moment envelopes, although the amplitudes vary.

Several cases were repeated for an H/L ratio of 1/5.0. The results indicated insignificant changes in the amplitude and shape of the moment envelopes.

Figures 24 through 31 show the graphs of the rib and tie moment influence lines for four of the $I_R/I_T = 1/10$ cases, for different hanger spacings. The H/L ratio for all cases is 1/5.9. The results indicate that the live load moment envelope does not change significantly for different hanger spacings.

By using Figures 18 through 31 the loading cases for maximum rib and tie live load moment can be determined. The results are shown in Table 3.

Table 3. Locations of maximum rib and tie live load moment.

Case No.	Rib or Tie	Distributed Load				Concentrated Load			
		Positive		Negative		Positive		Negative	
		ξ	L_P	ξ	L_N	η	L_P	η	L_N
1/20-16	Rib	0.38	0.25	0.56	0.75	0.19	0.19	0.31	0.75
	Tie	0.38	0.25	0.56	0.75	0.19	0.19	0.31	0.75
1/10-10	Rib	0.40	0.30	0.50	0.80	0.20	0.20	0.30	0.70
	Tie	0.40	0.20	0.50	0.80	0.20	0.20	0.30	0.70
1/10-12	Rib	0.42	0.25	0.50	0.75	0.25	0.25	0.33	0.75
	Tie	0.42	0.25	0.50	0.75	0.17	0.17	0.33	0.75
1/10-20	Rib	0.40	0.25	0.55	0.75	0.20	0.20	0.30	0.75
	Tie	0.40	0.25	0.55	0.75	0.20	0.20	0.30	0.75
1/10-24	Rib	0.42	0.25	0.54	0.75	0.21	0.21	0.29	0.71
	Tie	0.42	0.25	0.54	0.75	0.21	0.21	0.29	0.75
1-16	Rib	0.38	0.25	0.56	0.75	0.19	0.19	0.31	0.75
	Tie	0.38	0.25	0.56	0.75	0.19	0.19	0.31	0.75
20-16	Rib	0.38	0.25	0.56	0.75	0.19	0.19	0.31	0.75
	Tie	0.38	0.19	0.56	0.81	0.19	0.25	0.31	0.75

where:

L_P = Location of maximum positive live load moment, as a fraction of the span length L

L_N = Location of maximum negative live load moment, as a fraction of the span length L

η and ξ are fractions of the span length L as shown:

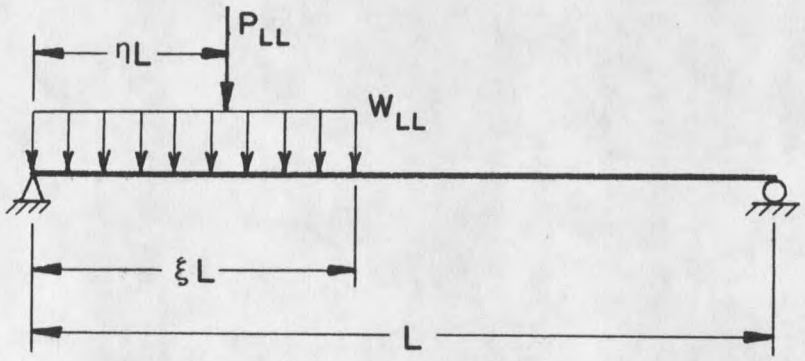

The absolute maximum rib and tie moments may not occur at a hanger location, but between them. This is due to the dead load of the members. Table 3 indicates that maximum positive live load moment occurs between the 0.20 and 0.25 points of a span. Maximum negative live load moment occurs near the 0.75 point. Therefore the flanges of the rib and tie might require larger areas in these portions of a span.

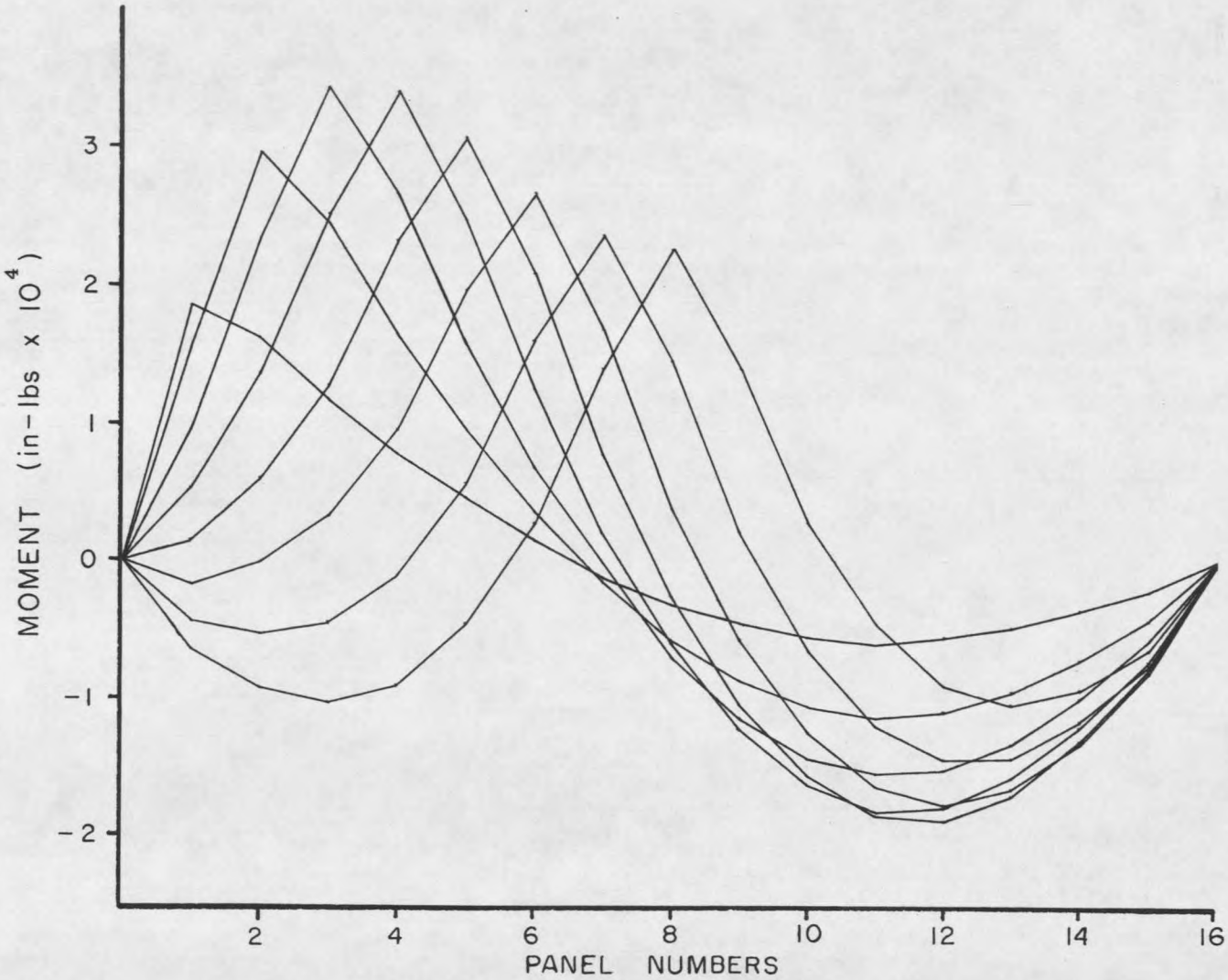

Figure 18. Graph of rib moment influence lines.
$A_R/A_T = 0.6$; $I_R/I_T = 1/20$; 16 Panels

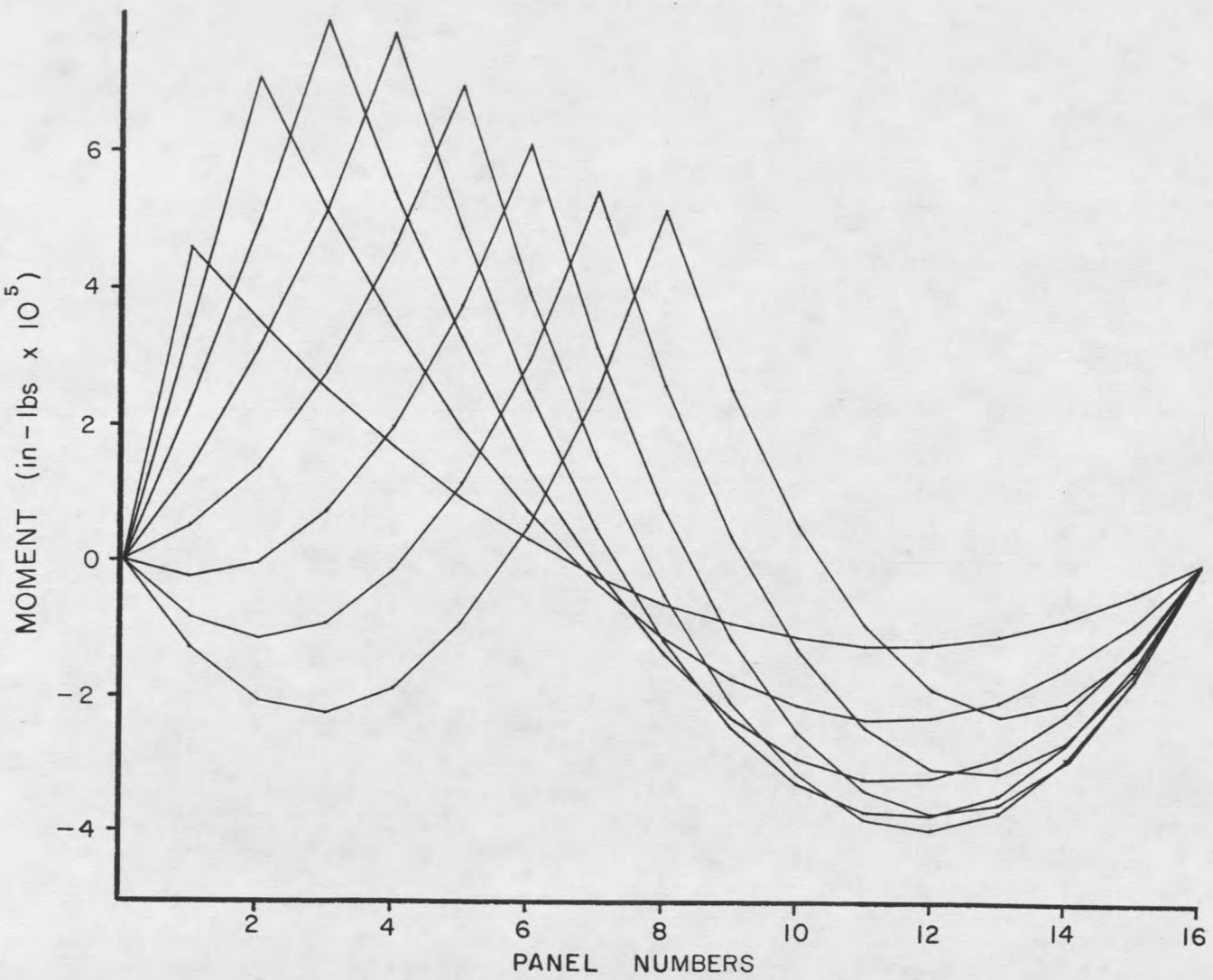

Figure 19. Graph of tie moment influence lines.
$A_R/A_T = 0.6$; $I_R/I_T = 1/20$; 16 Panels

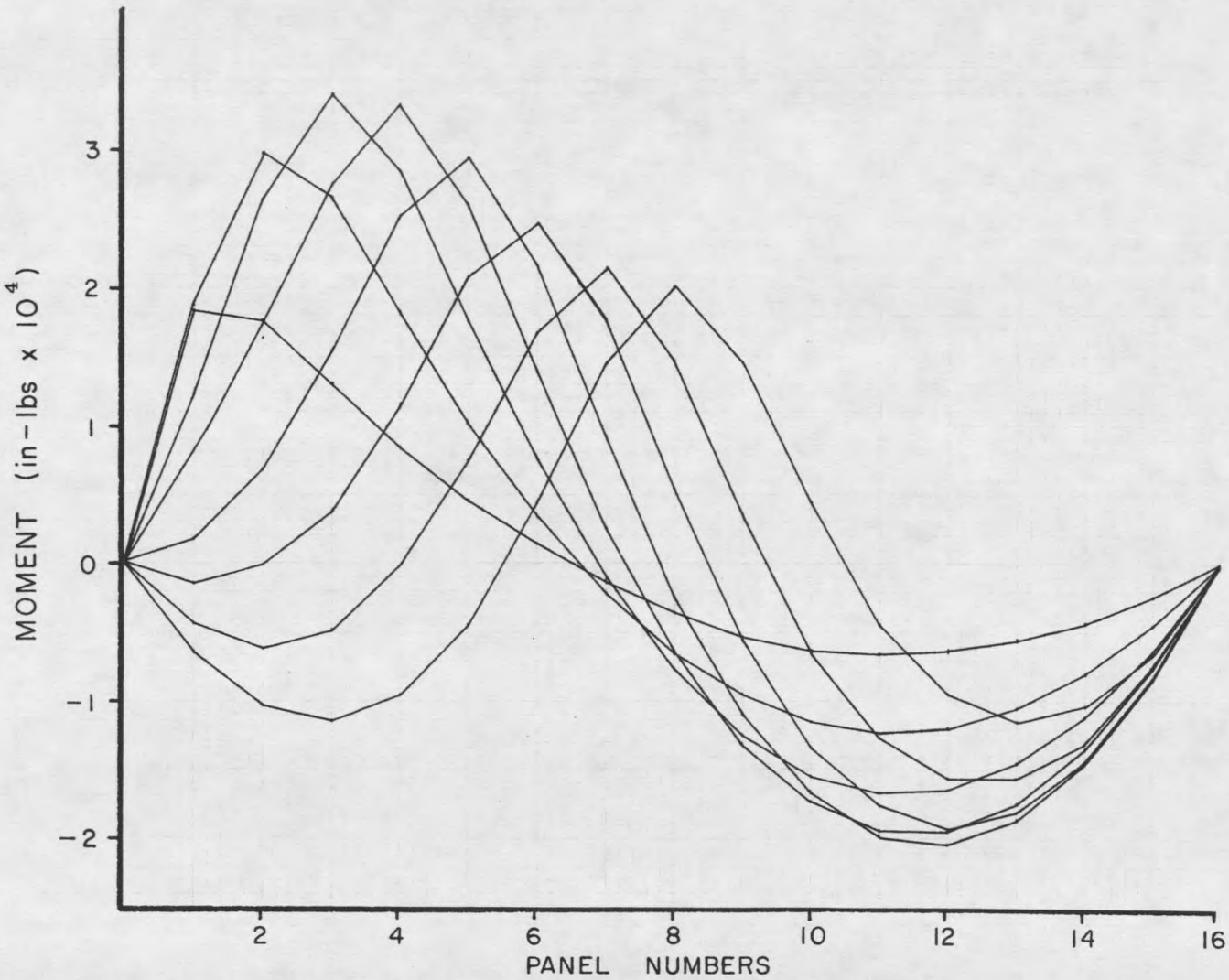

Figure 20. Graph of rib moment influence lines.
$A_R/A_T = 1.0$; $I_R/I_T = 1.0$; 16 Panels

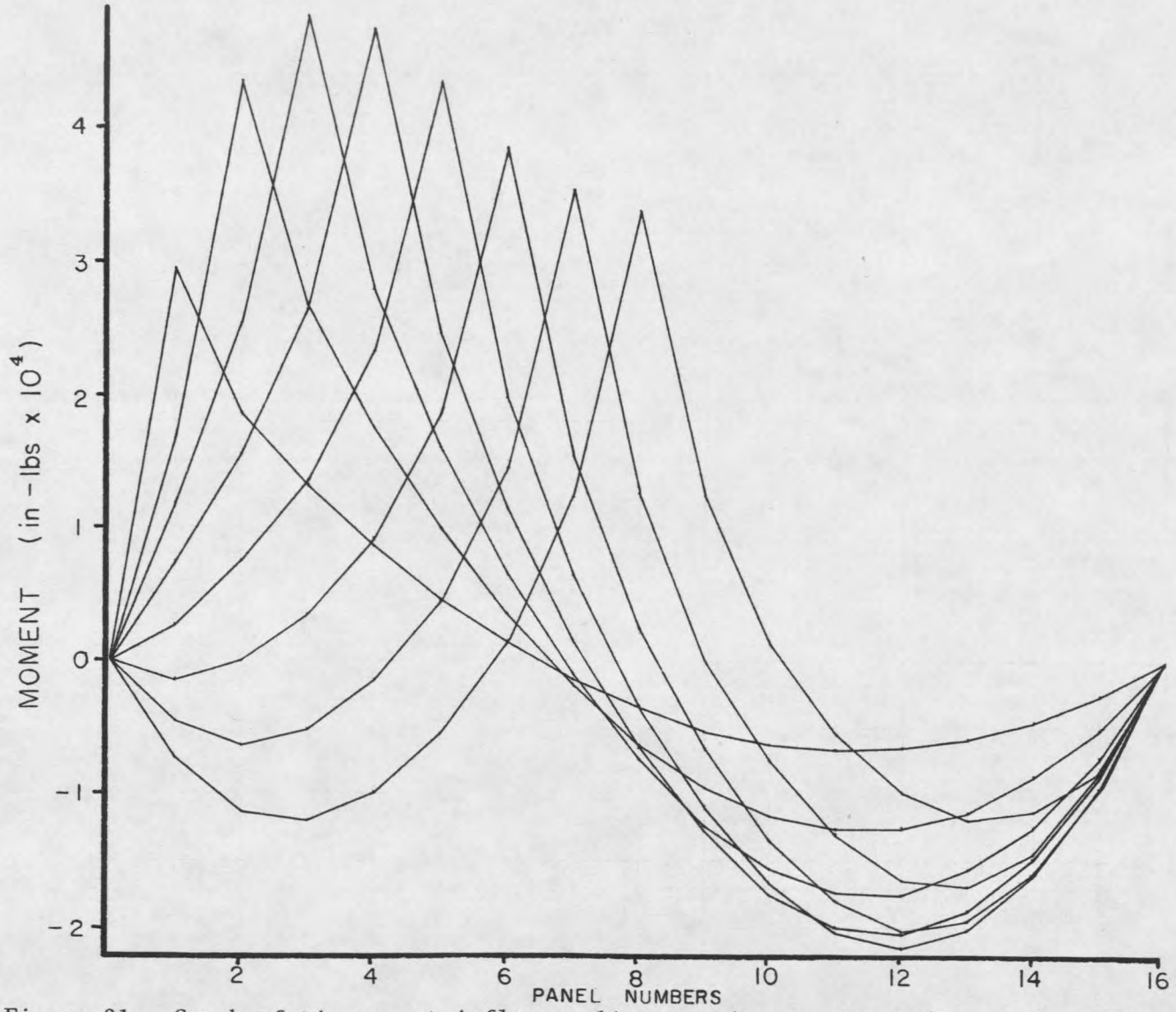

Figure 21. Graph of tie moment influence lines. $A_R/A_T = 1.0$; $I_R/I_T = 1.0$; 16 Panels

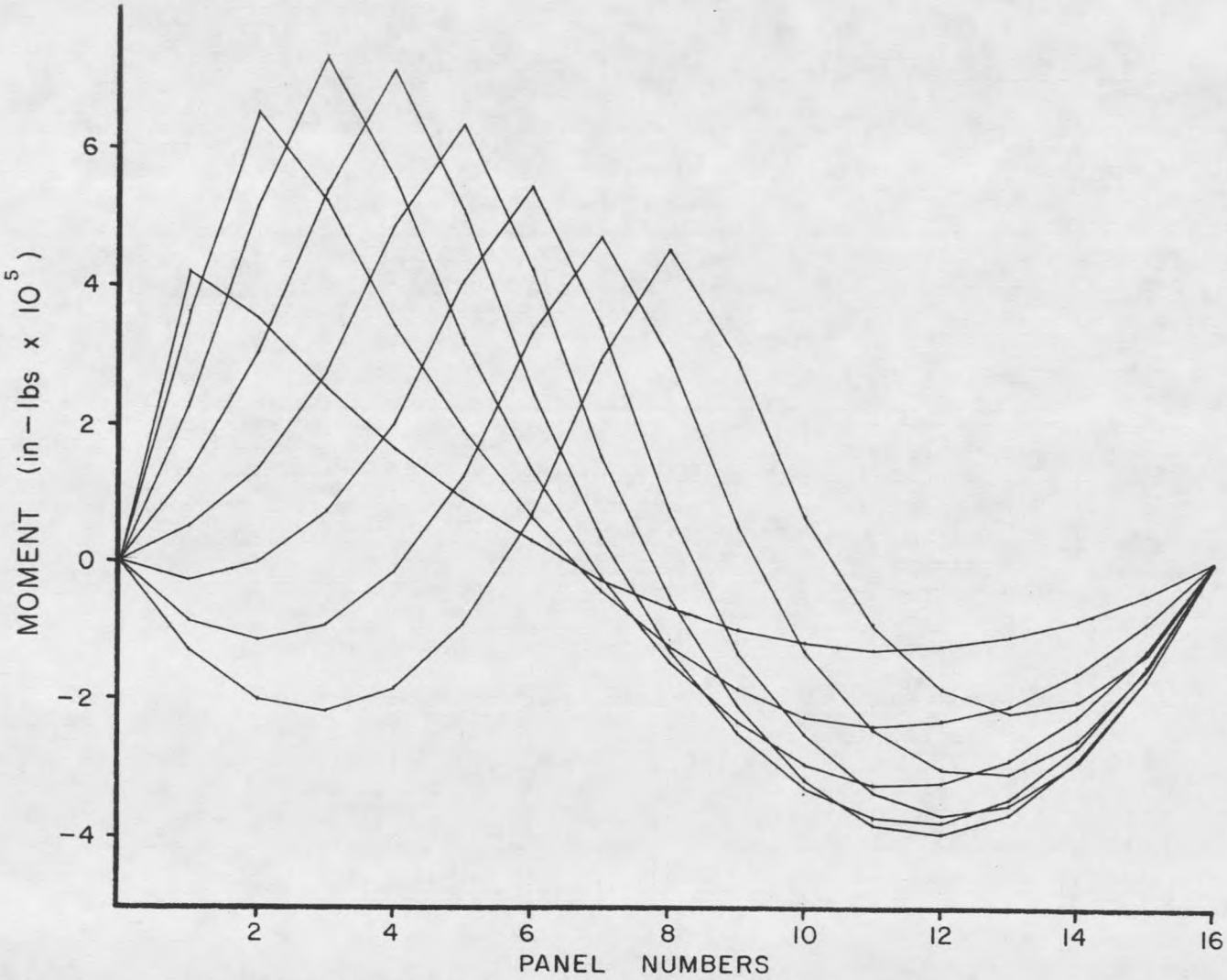

Figure 22. Graph of rib moment influence lines.
$A_R/A_T = 1.5$; $I_R/I_T = 20$; 16 Panels

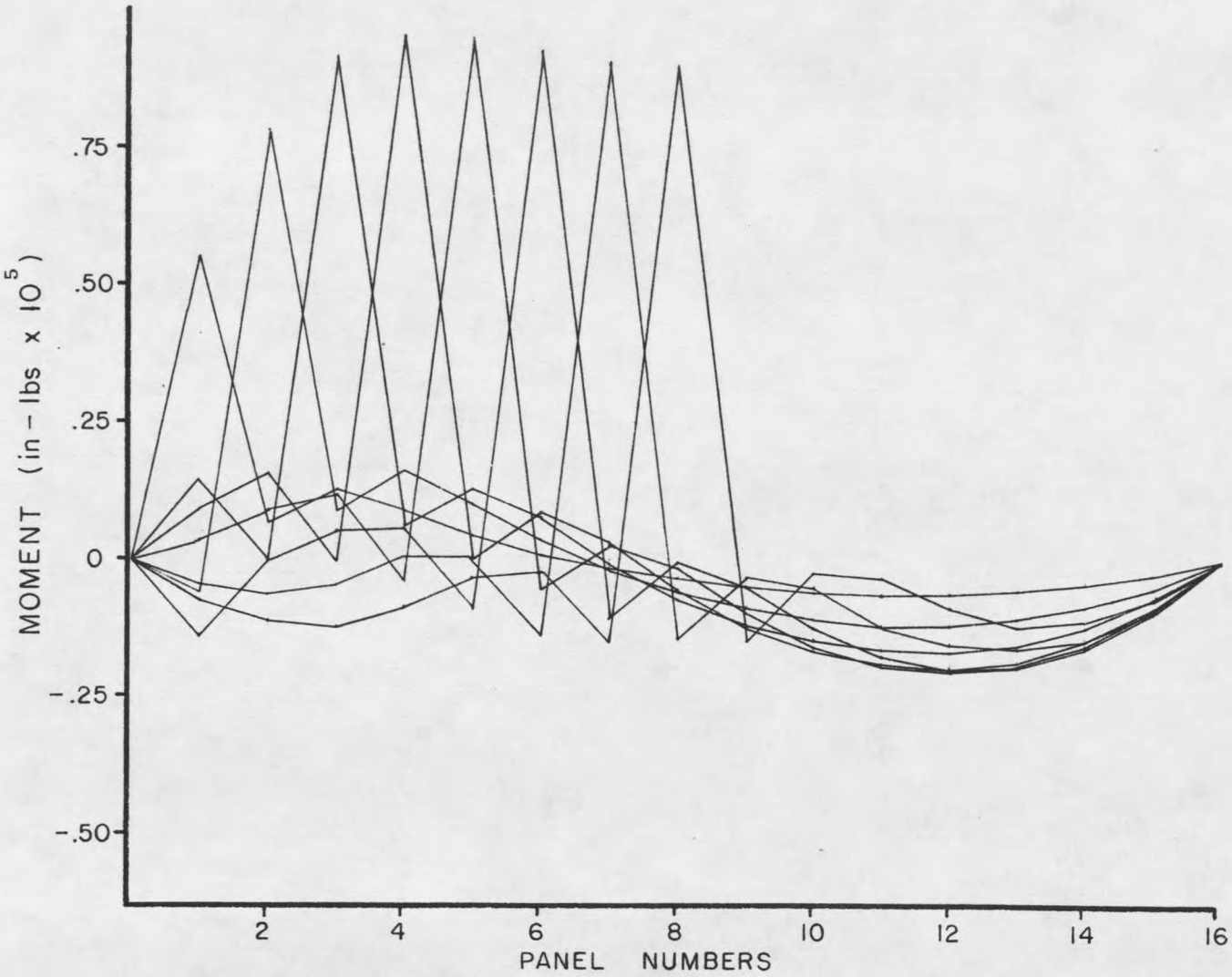

Figure 23. Graph of tie moment influence lines.
$A_R/A_T = 1.5$; $I_R/I_T = 20$; 16 Panels

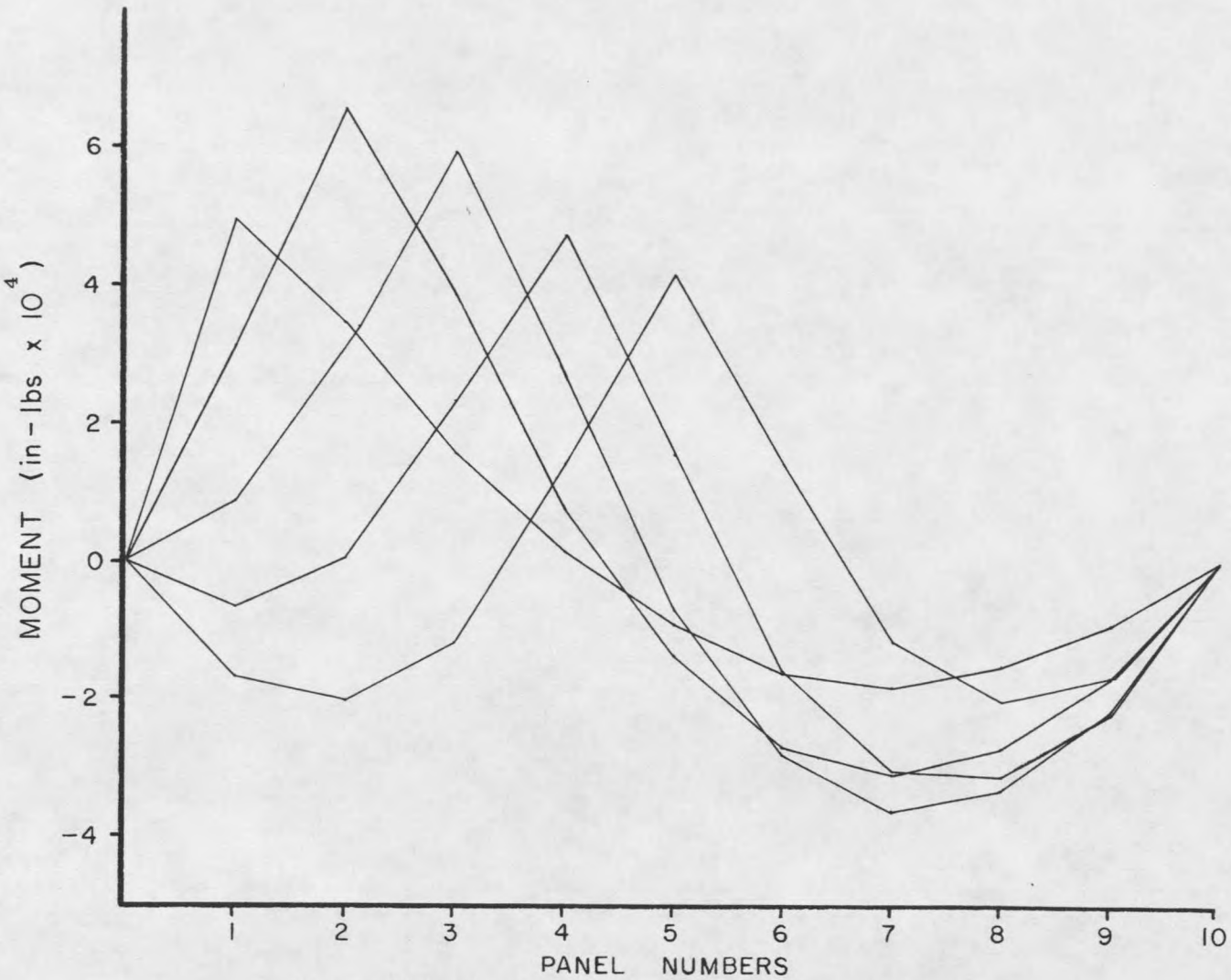

Figure 24. Graph of rib moment influence lines.
A_R/A_T = 1.0 ; I_R/I_T = 1/10 ; 10 Panels

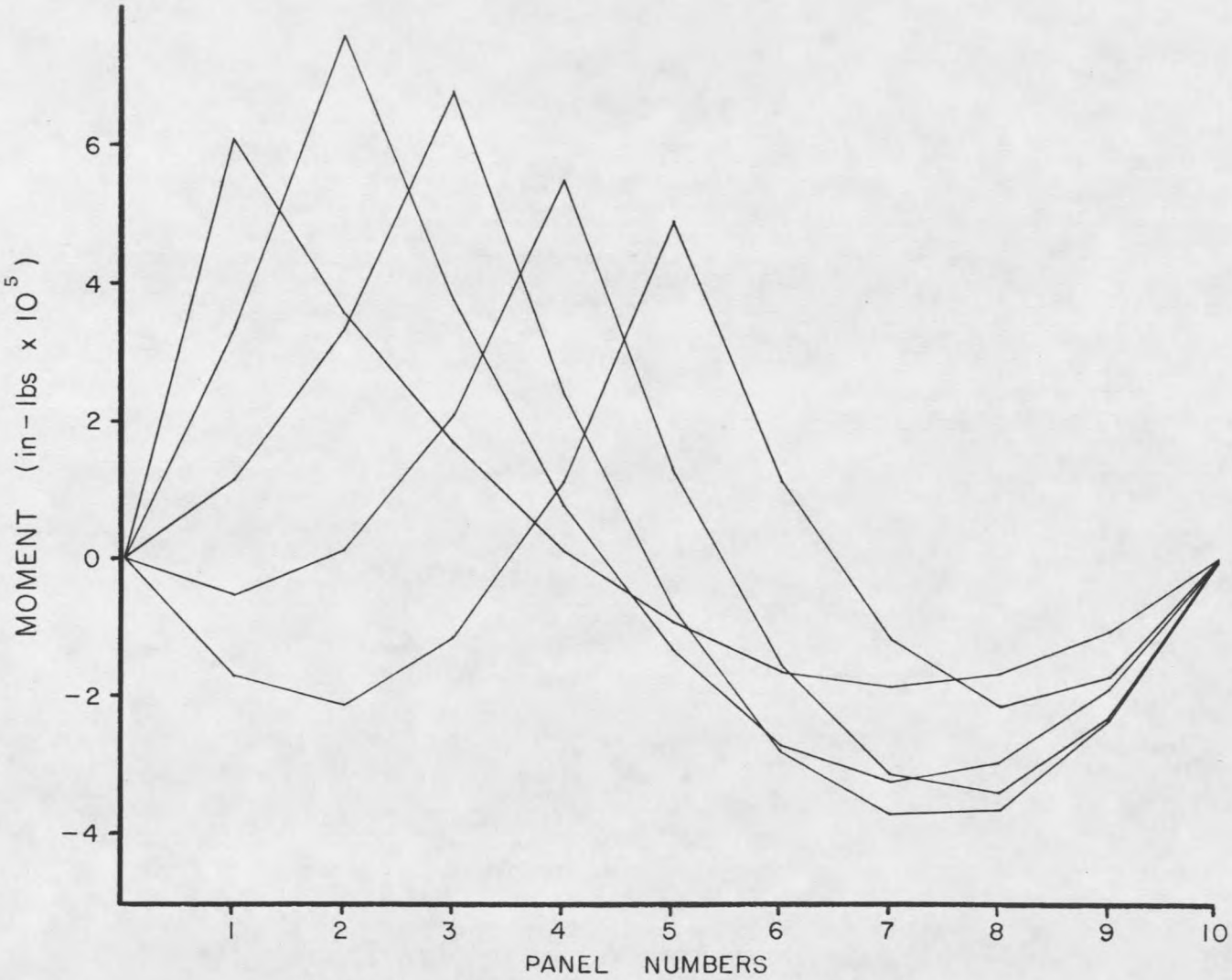

Figure 25. Graph of tie moment influence lines.
A_R/A_T = 1.0 ; I_R/I_T = 1/10 ; 10 Panels

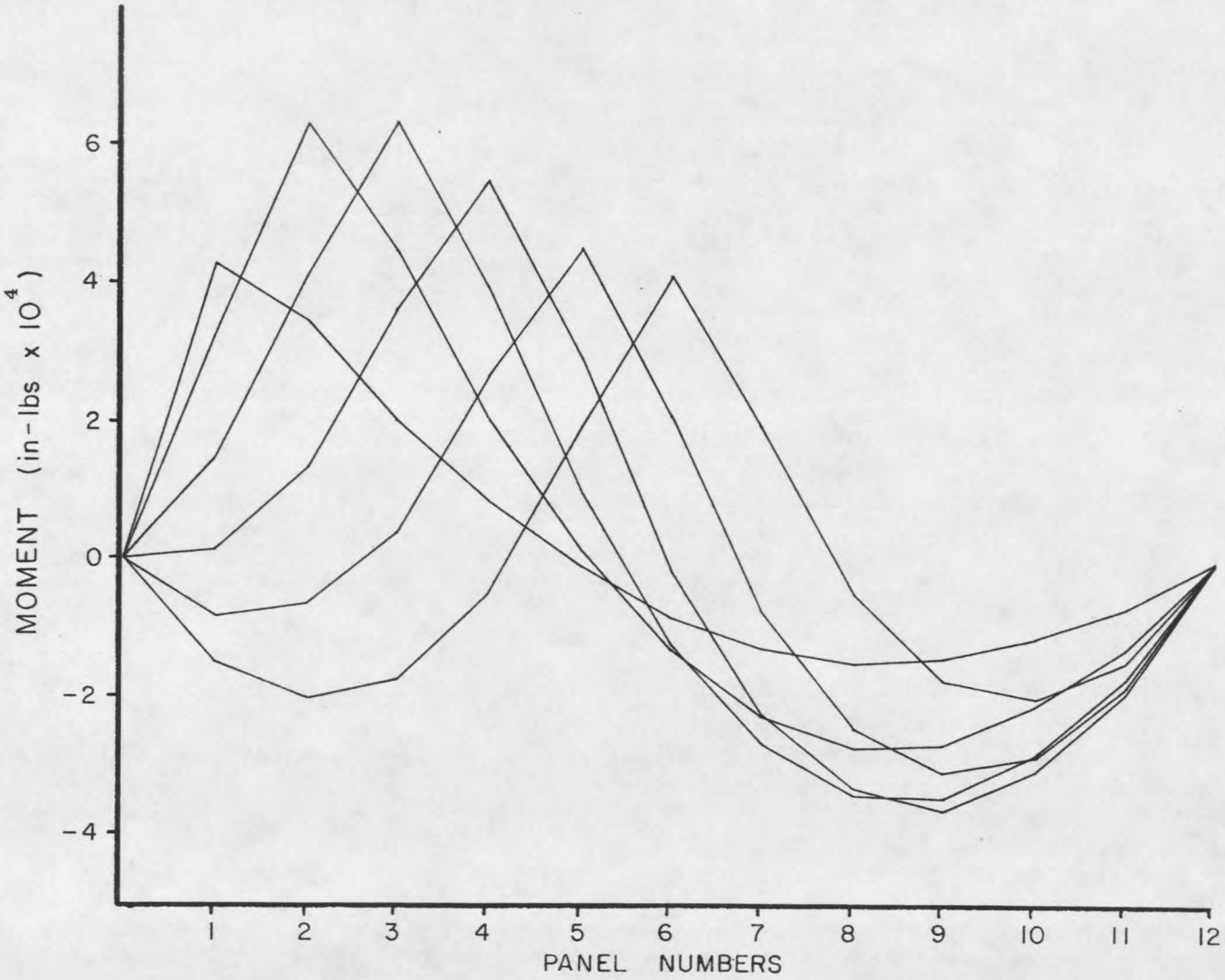

Figure 26. Graph of rib moment influence lines.
$A_R/A_T = 1.0$; $I_R/I_T = 1/10$; 12 Panels

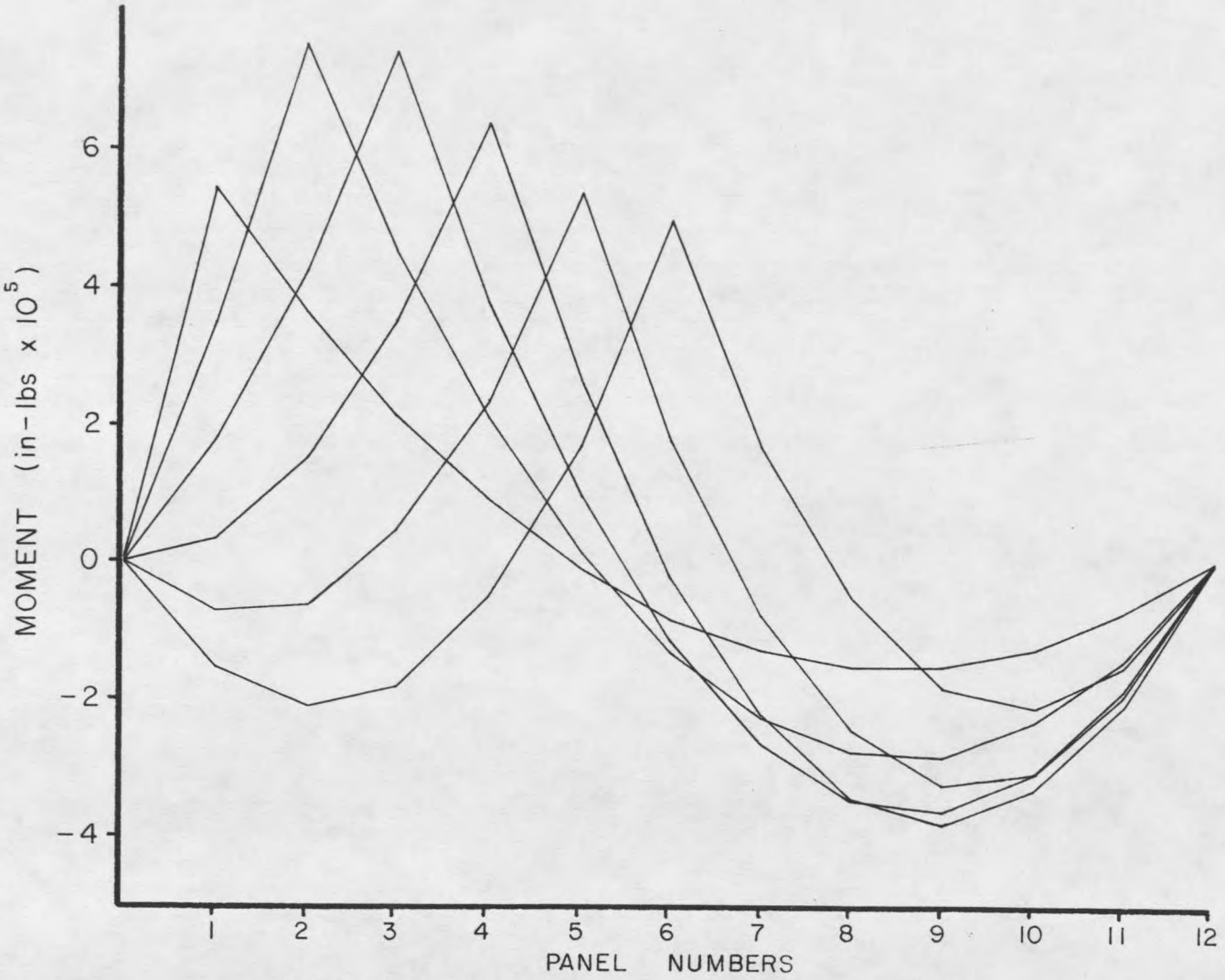

Figure 27. Graph of tie moment influence lines.
A_R/A_T = 1.0 ; I_R/I_T = 1/10 ; 12 Panels

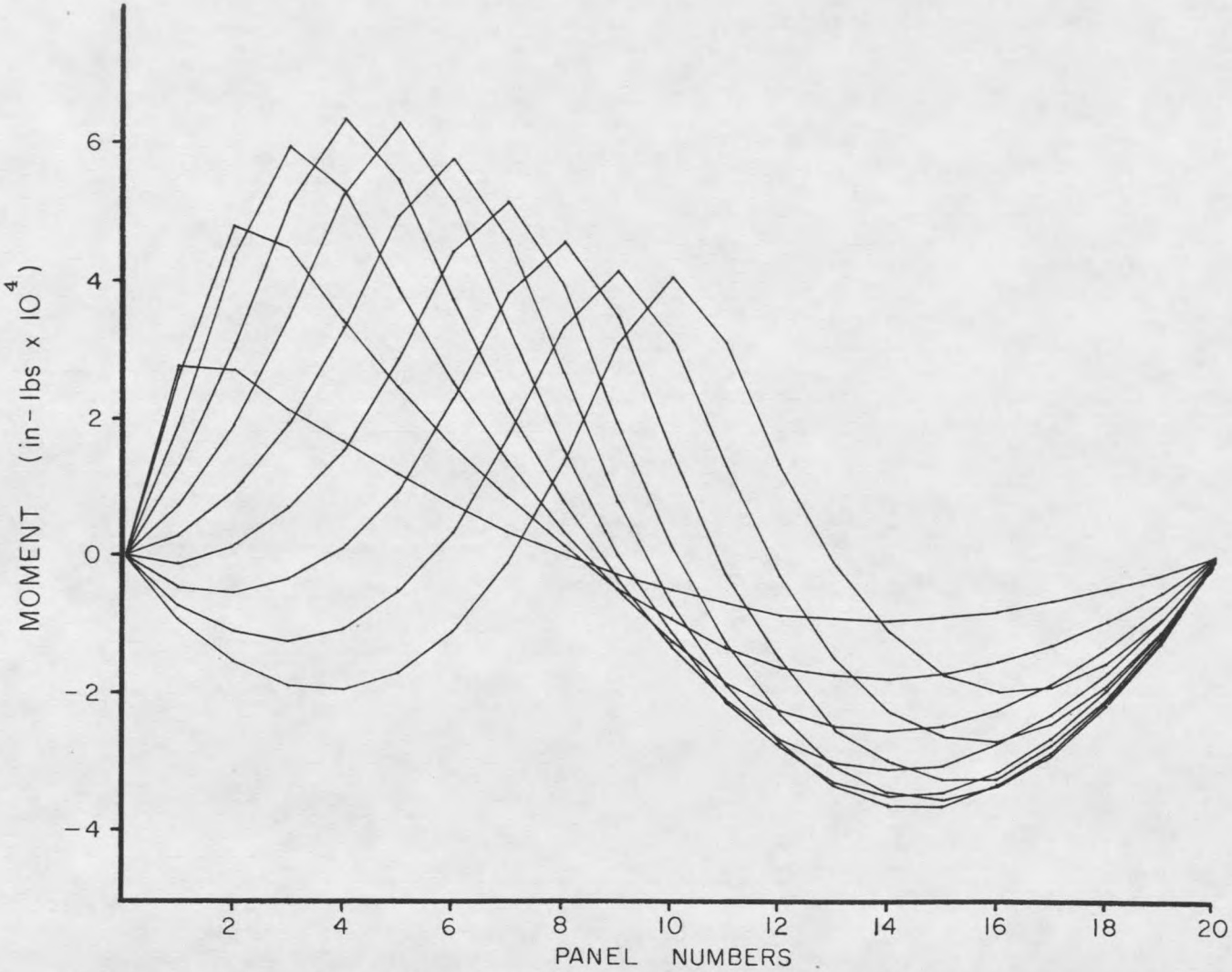

Figure 28. Graph of rib moment influence lines.
A_R/A_T = 1.0 ; I_R/I_T = 1/10 ; 20 Panels

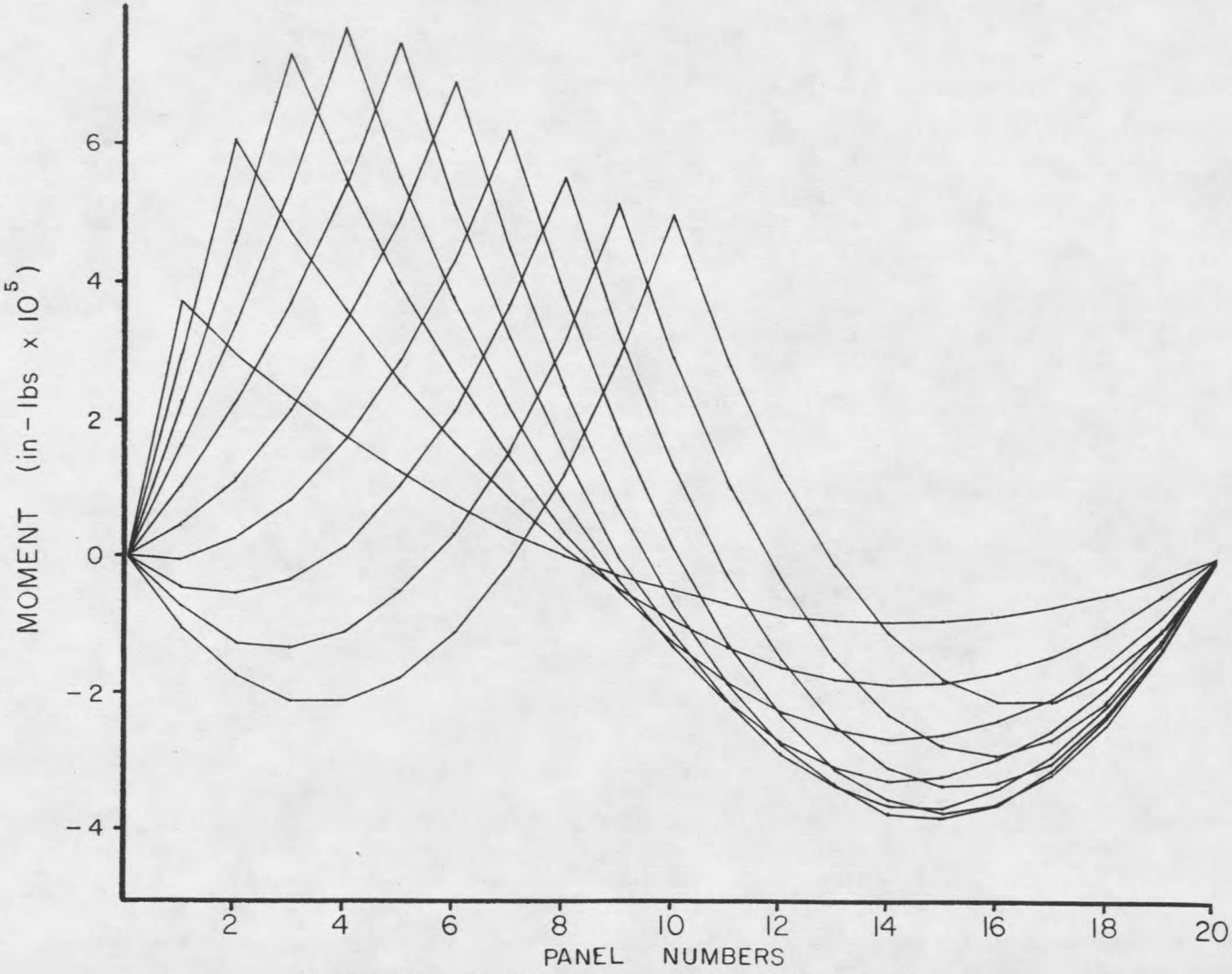

Figure 29. Graph of tie moment influence lines.
A_R/A_T = 1.0 ; I_R/I_T = 1/10 ; 20 Panels

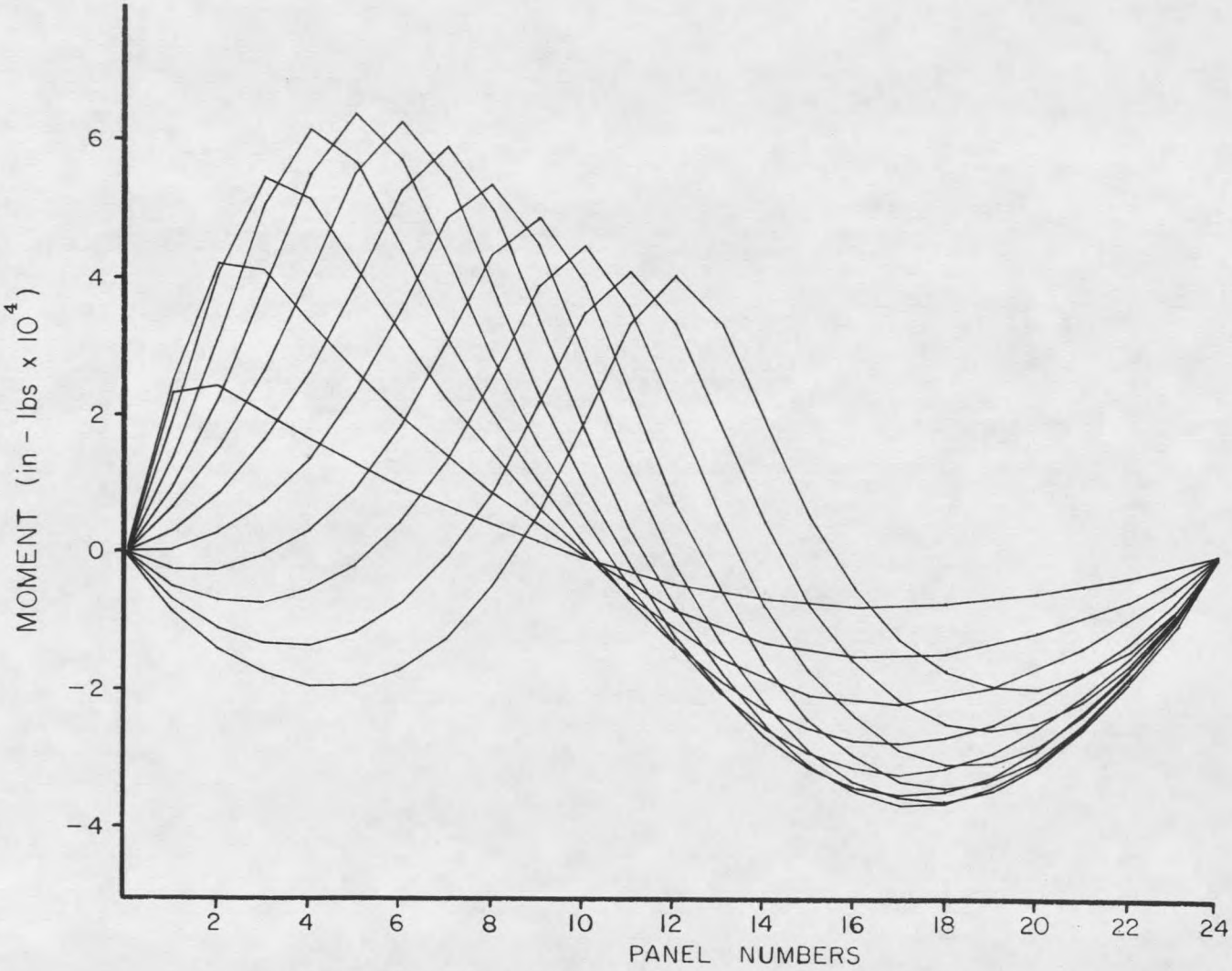

Figure 30. Graph of rib moment influence lines.
A_R/A_T = 1.0 ; I_R/I_T = 1/10 ; 24 Panels

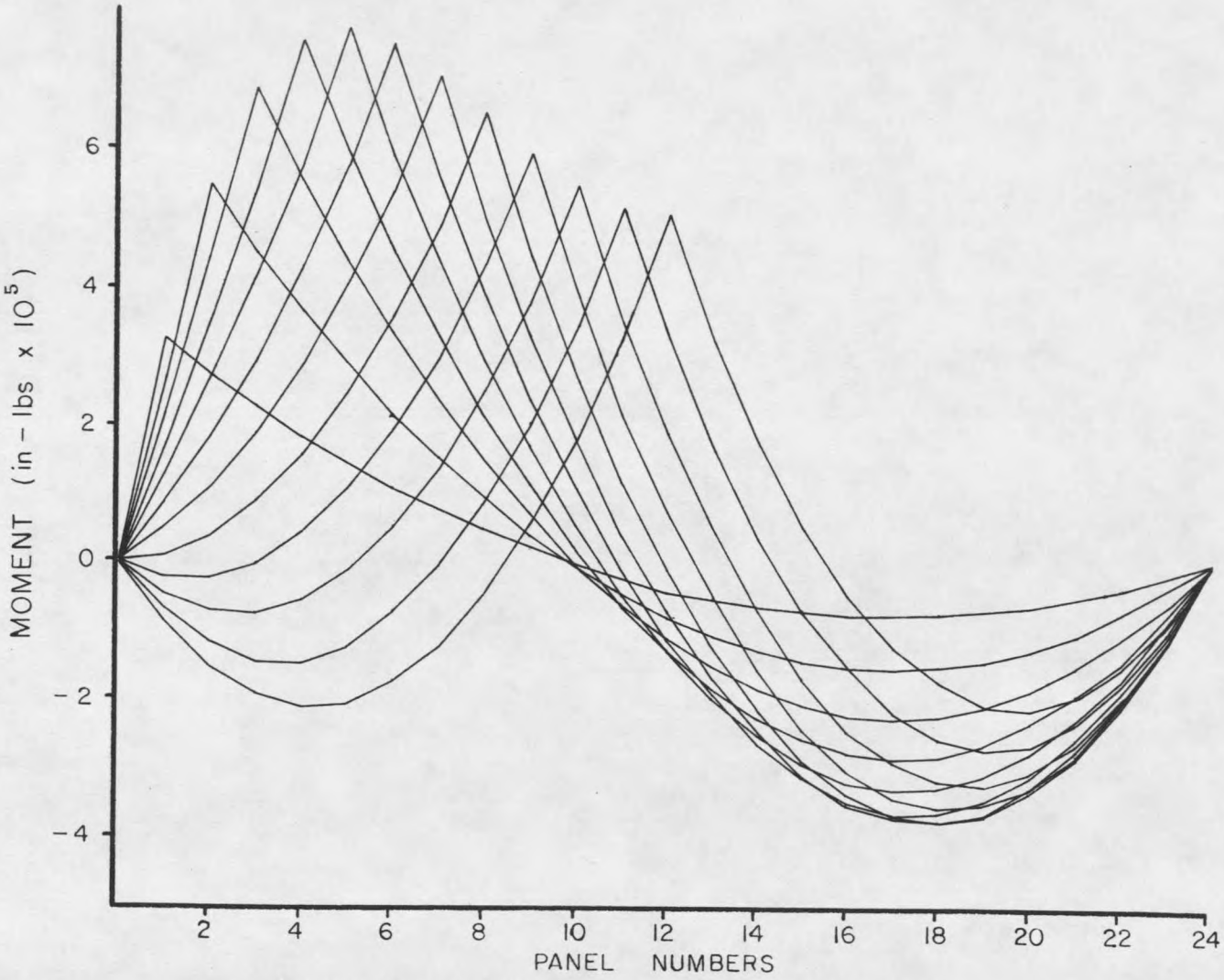

Figure 31. Graph of tie moment influence lines.
$A_R/A_T = 1.0$; $I_R/I_T = 1/10$; 24 Panels

Hanger Forces

The live load forces carried by the hangers in a tied arch are highly dependent upon the I_R/I_T ratio and the hanger spacing. The percentage of load carried into the hangers due to application of loads directly under the hangers were computed for several of the cases. The results for the hangers carrying the largest percentage of load are listed in Table 4, and graphed in Figures 32 and 33.

Table 4. Hangers carrying maximum force due to live load.

Case No.	H/L	ψ (Pct.)	Hanger Location
1/20-16	1/5.0	12.50	Center
1/20-16	1/5.9	12.60	Center
1/10-10	1/5.9	21.60	Center
1/10-12	1/5.9	18.50	Center
1/10-16	1/5.9	14.40	Center
1/10-20	1/5.9	11.80	Center
1/10-24	1/5.9	10.10	Center
1-16	1/5.0	27.00	Center
1-16	1/5.9	28.00	Center
20-16	1/5.0	74.60	Second from end
20-16	1/5.9	77.00	Second from end

where:

ψ = Percentage of a unit load carried by a hanger due to application of a unit load at the hanger

Figure 32 shows that for a bridge with a stiff rib and slender tie, most of the live load is transmitted into the hangers. The hanger forces decrease towards the center of the bridge. This occurs because the relative stiffness of the rib to tie decreases towards the center of the bridge. The case of the smaller H/L ratio only increased the hanger forces by about 3-1/2%.

Similarly, Figure 32 shows that for a bridge with a stiff tie and slender rib most of the live load is carried by bending moment in the tie. The hanger forces increase towards the center of the bridge. This is due to being away from the ends of the bridge where the relative stiffness of the rib to tie increases. The hanger forces were virtually unaffected by changes in the H/L ratio for the 1/20-16 cases.

When the size effects of the large joint between the rib and the tie are taken into account, the tensions in the end hangers decrease. This is due to the increased stiffness of the arch due to the joint.

Figure 33 demonstrates the effect of hanger spacing upon hanger forces, for the I_R/I_T = 1/10 cases. Increasing the hanger spacing for a given I_R/I_T ratio increases the hanger forces.

From this analysis it becomes apparent that for bridges with deep ties and shallow ribs, the critical hanger carrying maximum live load force is the center hanger. The loading to produce the maximum force would be a uniform load across the bridge, with a concentrated load at the center, or the maximum floor beam reaction could be used. An initial estimate of the maximum hanger force can be obtained from the relationship:

$$T_{max} = \frac{8ShM_L}{L^2(H-h)} + qS + \psi P + T_{DL} \quad (26)$$

where:

S = Distance between hangers
q = Uniform live load across the span
P = Concentrated live load applied at center hanger
h = Height of tie at centerspan
L = Length of span
ψ = Coefficient estimated from Table 4
H = Height of rib at centerspan
T_{DL} = Hanger tension due to dead load (Found from Equation (7).)
M_L = Internal arch live load moment at the center of the bridge

The critical hanger carrying maximum live load force for bridges with deep ribs and shallow ties, was the second hanger from either end. For bridges with wide hanger spacings the end hanger could be the critical hanger. The stiffness and size of the joint connecting the rib and tie would affect this.

The loading necessary to provide the maximum hanger force for this case would be a uniform load across the span, and a concentrated load applied at the second hanger from the end. An estimate of the hanger force can be obtained from Equation (26).

Values of ψ can be roughly interpolated from Table 4 for various values of I_R/I_T, and different hanger spacings. For example, if I_R/I_T = 1/8 and s = 12, the value of ψ could be estimated at 0.21. For I_R/I_T = 1/10 and s = 12, ψ would be 0.19. For bridges with deep ties, a conservative value of ψ would be 0.3.

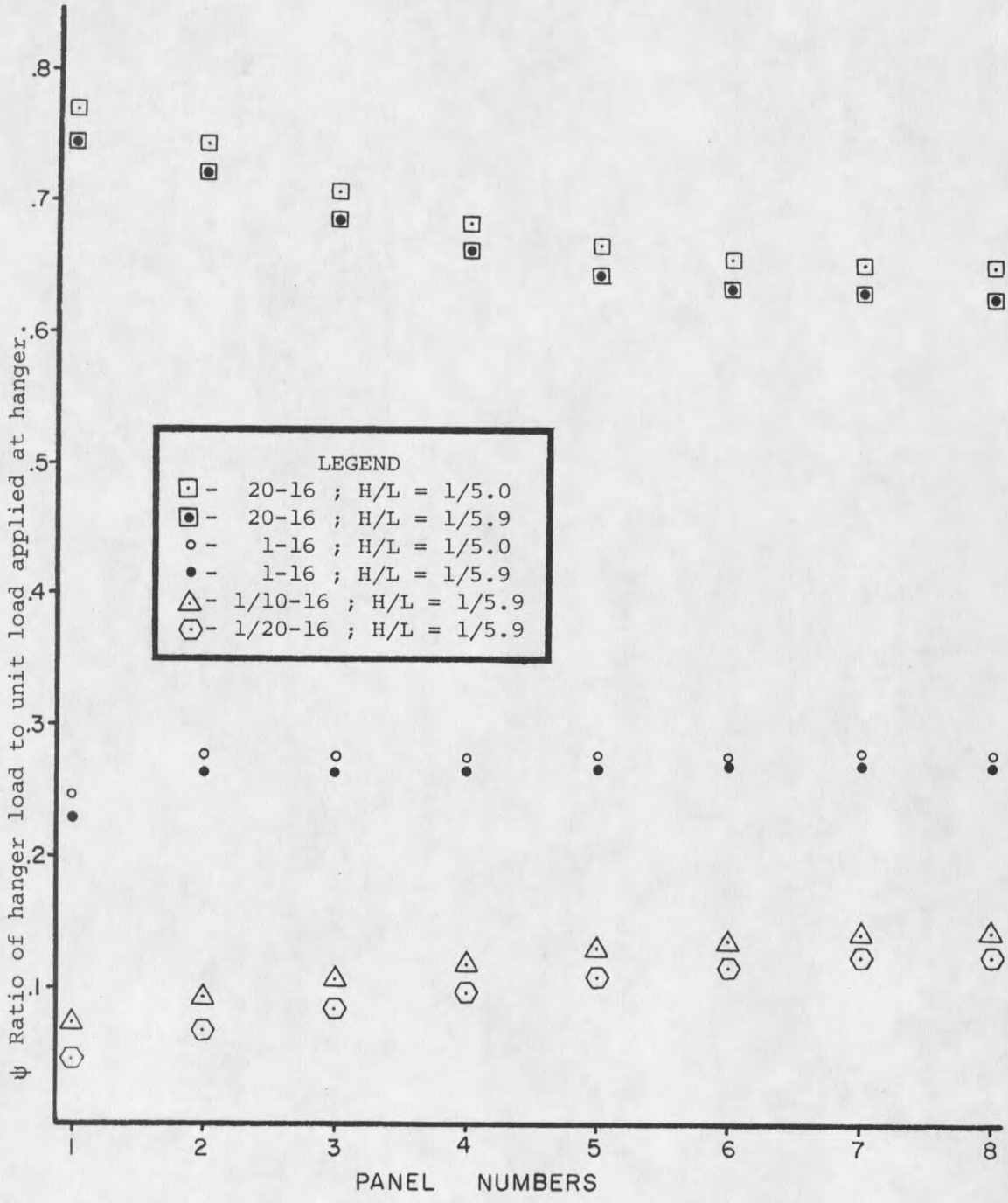

Figure 32. Graph showing effect of I_R/I_T ratio upon hanger forces.

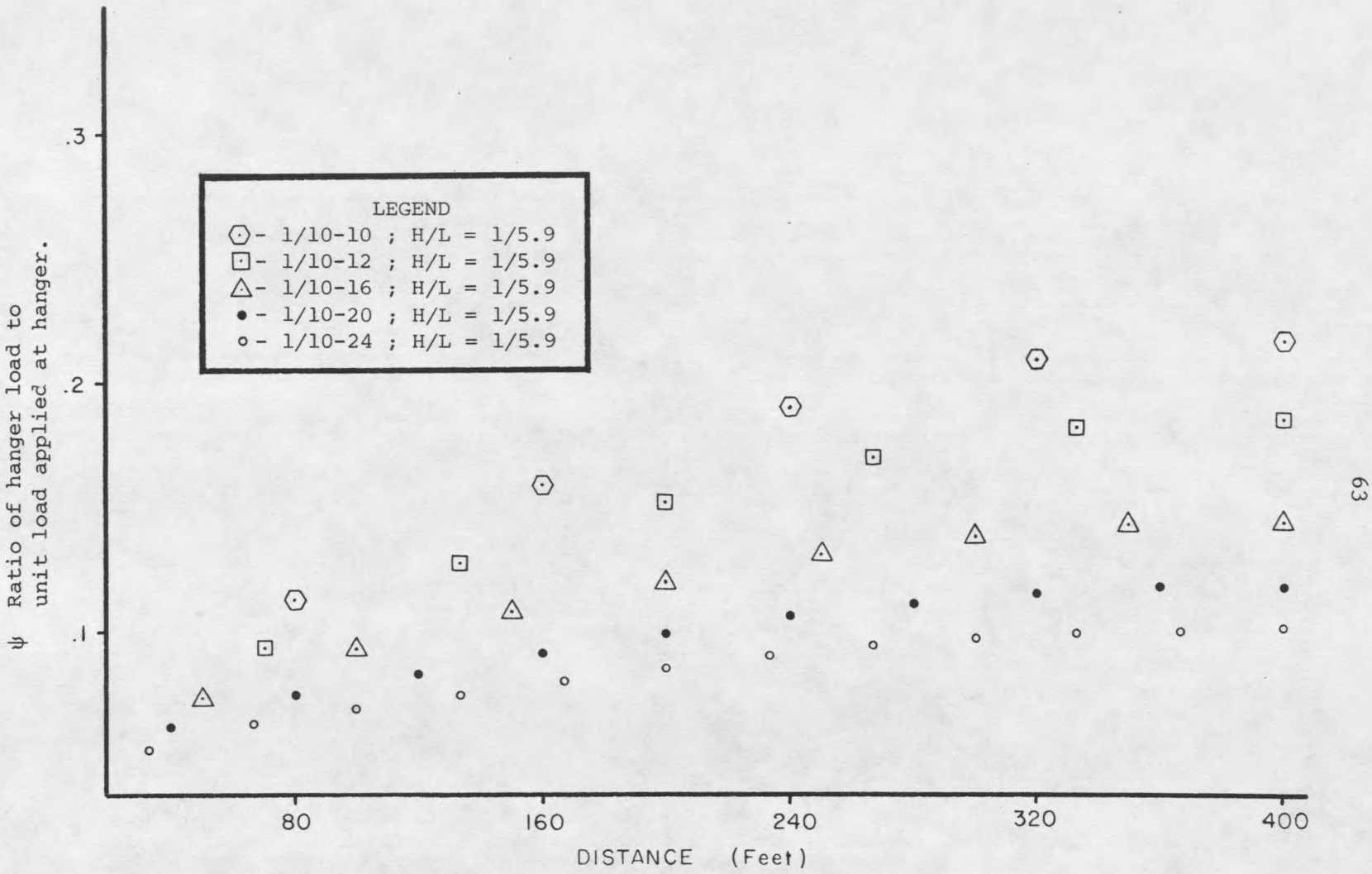

Figure 33. Graph showing effect of hanger spacing upon hanger forces.

Rib and tie deflection

For the s = 16 spacing case the following half span loading was used:

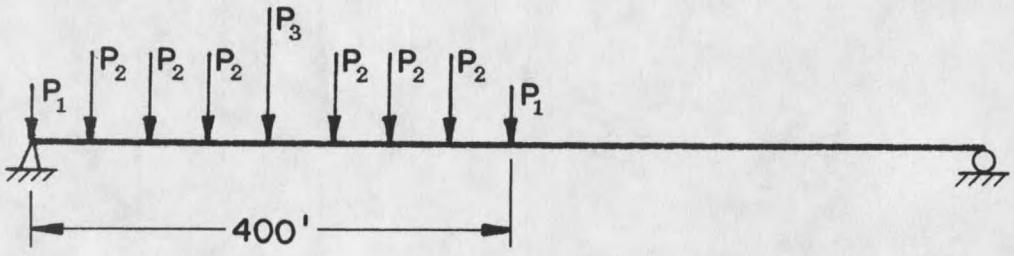

where:

P_1 = 22.5 kips
P_2 = 45.0 kips
P_3 = 70.2 kips

It was found that the largest live load deflection occurred under half span loading, with a concentrated load near the 0.25 point. Graphs of the rib and tie deflections are shown in Figures 34 and 35. The graphs show similar deflections for the rib and tie for a wide range of the various parameters. This verifies the classical theory of tied arches in assuming hanger elongation negligible compared with the rib and tie deflection, [7, 30]. Therefore for a given span length, loading, and cross-sectional area, the live load deflections are rather insensitive to changes in the I_R/I_T, A_R/A_T, or H/L ratios. The point of inflection also remained nearly unchanged, near the center of the arch.

Two additional cases were tried for determining deflections. The 1/20-16 and 20-16 cases were analyzed with the total cross-sectional

area of the arch reduced by one-half, to 300 in^2. the results indicate that the deflections still did not change drastically. The deflection increased for the loaded segment, and decreased for the unloaded segment. In addition, the point of inflection shifted to the right.